Inorg. Chem. **2003**, *42*, 1282−1295

Platinum and Palladium Imido and Oxo Complexes with Small Natural Bite Angle Diphosphine Ligands

U. Anandhi, Todd Holbert, Dennis Lueng, and Paul R. Sharp*

125 Chemistry, University of Missouri, Columbia, Missouri 65211

Received August 29, 2002

Treatment of L_2MCl_2 (M = Pt, Pd; L$_2$ = $Ph_2PCMe_2PPh_2$ (dppip), $Ph_2PNMePPh_2$ (dppma)) with AgX (X = OTf, BF_4, NO_3) in wet CH_2Cl_2 yields the dinuclear dihydroxo complexes $[L_2M(\mu\text{-OH})]_2(X)_2$, the mononuclear aqua complexes $[L_2M(OH_2)_2](X)_2$, the mononuclear anion complexes L_2MX_2, or mixtures of complexes. Addition of aromatic amines to these complexes or mixtures gives the dinuclear diamido complexes $[L_2Pt(\mu\text{-NHAr})]_2(BF_4)_2$, the mononuclear amine complexes $[L_2M(NH_2Ar)_2](X)_2$, or the dinuclear amido–hydroxo complex $[Pt_2(\mu\text{-OH})(\mu\text{-NHAr})(dppip)_2](BF_4)_2$. Deprotonation of the Pd and Pt amine or diamido complexes with M′N(SiMe$_3$)$_2$ (M′ = Li, Na, K) gives the diimido complexes $[L_2M(\mu\text{-NAr})]_2$ associated with M′ salts. Structural studies of the Li derivatives indicate association through coordination of the imido nitrogen atoms to Li^+. Deprotonation of the amido–hydroxo complex gives the imido–oxo complex $[Pt_2(\mu\text{-O})(\mu\text{-NAr})(dppip)_2]\cdot LiBF_4\cdot LiN(SiMe_3)_2$, and deprotonation of the dppip Pt hydroxo complex gives the dioxo complex $[Pt(\mu\text{-O})(dppip)]_2\cdot LiN(SiMe_3)_2\cdot 2LiBF_4$.

Introduction

Interest in the chemistry of late transition metals bonded to simple anionic oxygen- and nitrogen-containing ligands such as aryloxo, alkoxo, hydroxo, amido, oxo, and imido ligands derives from several areas including chemotherapy drugs,[1] enzyme modeling,[2] and various catalytic and stoichiometric processes.[3] Oxo and imido complexes are of particular interests since there is a scarcity of such complexes, especially in comparison to the early transition metals, and because of the perception that such scarcity implies high and/or unusual reactivity for these complexes.[3]

Our efforts have been directed at the synthesis of oxo and imido complexes of the heavier late transition metals Rh, Ir, Pd, Pt, and Au.[3b] We have reported oxo and imido complexes for all of these metals except Pd.[4] Application of successful techniques for Pt to the synthesis of the Pd analogues have generally failed, and analogous Pd oxo and imido complexes have remained elusive. Even for Pt, imido complexes have been difficult to obtain. Although a series of oxo complexes containing ancillary phosphine ligands have been prepared,[5] analogous imido complexes can only be isolated in the special case of the dppm ligand.[6] The synthesis of the dppm imido complexes is complicated by initial deprotonation of the methylene bridge of the dppm ligand (Scheme 1). As a result, the final deprotonation of the amido ligands is from a neutral complex instead of a dicationic complex. The absence of positive charge decreases

* To whom correspondence should be addressed. E-mail: SharpP@Missouri.edu.

(1) Reviews: (a) Berners-Price, S. J.; Appleton, T. G. *Platinum-Based Drugs Cancer Ther.* **2000**, 3−35. (b) Sherman, S. E.; Lippard, S. J. *Chem. Rev.* **1987**, *87*, 1153−1181. (c) *Platinum, Gold, and Other Metal Chemotherapeutic Agents: Chemistry and Biochemistry*; Lippard, S. J., Ed.; American Chemical Society: Washington, DC, 1983.

(2) Reviews: (a) Que, L., Jr.; Tolman, W. B. *Angew. Chem., Int. Ed.* **2002**, *41*, 1114−1137. (b) Holland, P. L.; Tolman, W. B. *Coord. Chem. Rev.* **1999**, *192*, 855−869. (c) Klinman, J. P. *Chem. Rev.* **1996**, *96*, 2541−2562. (d) Solomon, E. I.; Sundaram, U. M.; Machonkin, T. E. *Chem. Rev.* **1996**, *96*, 2563−2605. (e) Holm, R. H.; Kennepohl, P.; Solomon, E. I. *Chem. Rev.* **1996**, *96*, 2239−2314. (f) Solomon, E. I.; Tuczek, F.; Root, D. E.; Brown, C. A. *Chem. Rev.* **1994**, *94*, 827−856. (g) Karlin, K. D.; Tyeklar, Z. *Adv. Inorg. Biochem.* **1994**, *9*, 123−172. (h) Solomon, E. I.; Baldwin, M. J.; Lowery, M. D. *Chem. Rev.* **1992**, *92*, 521−542. (i) Karlin, K. D.; Gultneh, Y. *Prog. Inorg. Chem.* **1987**, *35*, 219−328.

(3) Reviews: (a) Cinellu, M. A.; Minghetti, G. *Gold Bull.* **2002**, *35*, 11−20. (b) Sharp, P. R. *J. Chem. Soc., Dalton Trans.* **2000**, 2647−2657. (c) Sharp, P. R. *Comments Inorg. Chem.* **1999**, *21*, 85−114. (d) Oro, L. A.; Ciriano, M. A.; Tejel, C.; Shi, Y.-M.; Modrego, J. *Metal Clusters Chem.* **1999**, *1*, 381−398. (e) Brunet, J.-J. *Gazz. Chim. Ital.* **1997**, *127*, 111−118. (f) Bergman, R. G. *Polyhedron* **1995**, *14*, 3227−3237. (g) Wigley, D. E. *Prog. Inorg. Chem.* **1994**, *42*, 239−482. (h) Fryzuk, M. D.; Montgomery, C. D. *Coord. Chem. Rev.* **1989**, *95*, 1−40. (i) Power, P. P. *Comments Inorg. Chem.* **1989**, *8*, 177−202. (j) West, B. O. *Polyhedron* **1989**, *8*, 219−274. (k) Bryndza, H. E.; Tam, W. *Chem. Rev.* **1988**, *88*, 1163−1188. (l) Griffith, W. P. *Coord. Chem. Rev.* **1970**, *5*, 459−517.

(4) The only reported Pd imido complex is trimeric $[Pd_3(NHPh)(NPh)_2(PEt_3)_3]^+$, unexpectedly isolated in poor yield from the reaction of $(PEt_3)_2PdCl_2$ with $[PhN_3NHCH_2CH_2NH]^{2-}$: Lee, S. W.; Trogler, W. C. *Inorg. Chem.* **1990**, *29*, 1099−1102.

(5) Li, J. J.; Li, W.; Sharp, P. R. *Inorg. Chem.* **1996**, *35*, 604−613.

(6) Li, J. J.; Li, W.; James, A. J.; Holbert, T.; Sharp, T. P.; Sharp, P. R. *Inorg. Chem.* **1999**, *38*, 1563−1572.

10.1021/ic025987f CCC: $25.00 © 2003 American Chemical Society
Published on Web 01/16/2003

Scheme 1

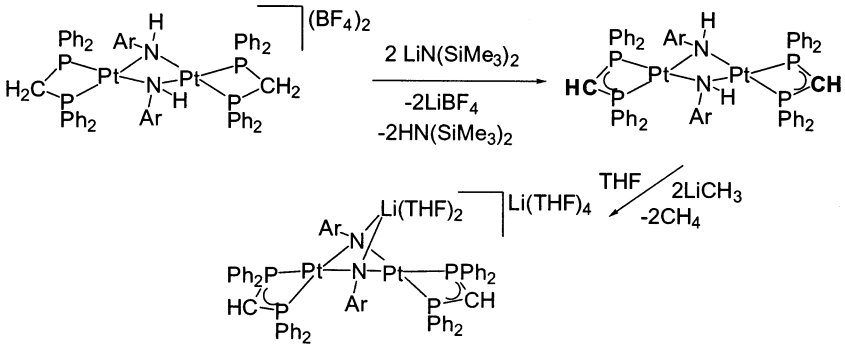

the acidity of the amido group N−H, and the final deprotonation to the anionic imido complex requires the strong base MeLi. In this report we present our results on a new series of Pt and Pd complexes with small natural bite angle diphosphine ligands related to dppm but which do not contain acidic hydrogen atoms. These smaller natural bite angle diphosphine ligands have allowed the facile preparation of a number of new Pt and Pd complexes including imido complexes for both Pt and Pd.

Results

Reactions of L_2PtCl_2 with $AgBF_4$. The hydroxo complexes $[L_2Pt(\mu\text{-}OH)_2]_2(BF_4)_2$ (**1**) (L_2 = $Ph_2PN(Me)PPh_2$ (dppma), $Ph_2PC(Me_2)PPh_2$ (dppip)) are prepared by treating L_2PtCl_2 with $AgBF_4$ (eq 1). The reactions are similar to those reported for related Pt(II) and Pd(II) phosphine complexes[7] including the closely related dppm complexes.[5]

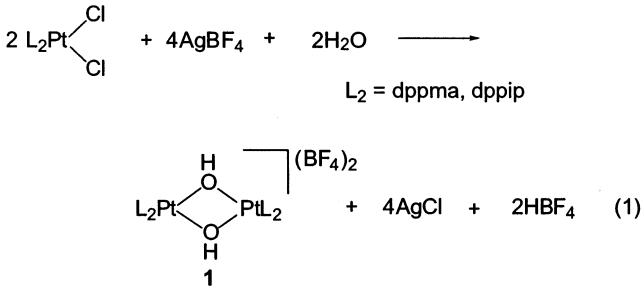

(1)

1

^{31}P NMR spectra of the reaction mixtures and isolated **1** show a singlet at 10.5 (dppma) or −30.5 (dppip) ppm flanked by ^{195}Pt satellites with J_{Pt-P} = 3483 (dppma) or 3125 (dppip) Hz. ^1H NMR spectra of **1** show bidentate phosphine ligand peaks in which the methyl groups appear as triplets with $^3J_{P-H}$ = 12.5 (dppma) or 15.0 (dppip) Hz. In addition to the phosphine ligand signals, signals for the bridged OH groups are observed at 3.02 (dppma) and 2.02 (dppip) ppm.

The successful formation of the hydroxo complexes depends on the amount of water present in the reaction mixture. In the case of L_2 = dppip, if water is present in too low an amount, the ^{31}P NMR spectrum of the reaction mixture and the isolated complex show an impurity peak at −29.1 ppm with a J_{Pt-P} coupling constant of 3140 Hz. The ^{31}P NMR spectrum of the reaction mixture when too much water is present shows a peak at −32.0 ppm (J_{Pt-P} = 3185 Hz). This coupling constant is 60 Hz more than the bridged hydroxo complex, and we attribute this signal to diaquo complex $[(dppip)Pt(OH_2)_2](BF_4)_2$.

In the case of L_2 = dppma, other complexes also form if water is not present in the correct amount. ^{31}P NMR spectra of the reaction mixtures and the isolated solids show additional broad peaks at 9.0 and 8.0 ppm when too much or too little water is present. Purification of the mixtures, to obtain selectively the hydroxo complex, was not successful.

The nitrate complex $Pt(dppma)(NO_3)_2$ (**2**), useful for the preparation of Pt mononuclear diamine complexes (see below), is obtained by treatment of $PtCl_2$(dppma) with $AgNO_3$ in dry CH_2Cl_2 (eq 2). The ^{31}P NMR spectrum of **2** shows an upfield singlet flanked by Pt satellites with larger coupling constants as compared to the chloro complexes. The ^1H NMR spectrum shows only peaks for the dppma ligand. Single-crystal X-ray analysis shows the structure given in Figure 1.[8] An abbreviated summary of crystal data and data collection and processing is given in Table 1. Selected bond distances and angles are listed in Table 3.

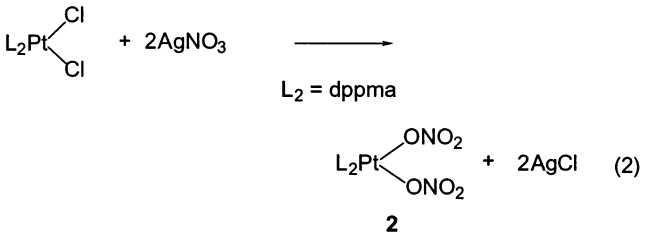

(2)

2

Reactions of L_2PdCl_2 with AgX. Analogous reactions of the Pd complexes $PdCl_2L_2$ give different products from those

(7) (a) Bushnell, G. W.; Dixon, K. R.; Hunter, R. G.; McFarland, J. J. *Can. J. Chem.* **1972**, *50*, 3694. (b) Rochon, F. D.; Guay, F. *Acta Crystallogr., Sect. C* **1987**, *43*, 43. (c) Trovo, G.; Bandoli, G.; Casellato, U.; Corain, B.; Nicolini, M.; Longata, B. *Inorg. Chem.* **1990**, *29*, 4616−4621. (d) Pisano, C.; Consiglio, G.; Sironi, A.; Moret, M. *J. Chem. Soc., Chem. Commun.* **1991**, 421−3. (e) Fallis, S.; Anderson, G. K.; Rath, N. P. *Organometallics* **1991**, *10*, 3180−3184. (f) Ericson, V.; Lovqvist, K.; Noren, B.; Oskarsson, A. *Acta Chem. Scand.* **1992**, *46*, 854. Ganguly, S.; Mague, J. T.; Roundhill, D. M. *Inorg. Chem.* **1992**, *31*, 3831−3835. (g) Rochon, F. D.; Melanson, R.; Morneau, A. *Magn. Reson. Chem.* **1992**, *30*, 697. (h) Bandini, A. L.; Banditelli, G.; Demartin, F.; Manassero, M.; Minghetti, G. *Gazz. Chim. Ital.* **1993**, *123*, 417−423. (i) Burgarcic, Z.; Lovqvist, K.; Oskarsson, A. *Acta Crystallogr., Sect. C* **1994**, *50*, 1028. (j) Miyamoto, T. K. *Chem. Lett.* **1994**, 1971. (k) Marvin, J. R.; Abbott, E. H. *Inorg. Chim. Acta* **1996**, *247*, 267−271. (l) Strukul, G.; Varagnolo, A.; Pinna, F. *J. Mol. Catal., A* **1997**, *117*, 413−423. (m) Gavagnin, R.; Cataldo, M.; Pinna, F.; Strukul, G. *Organometallics* **1998**, *17*, 661−667. (n) Fujii, A.; Hagiwara, E.; Sodeoka, M. *J. Am. Chem. Soc.* **1999**, *121*, 5450−5458. (o) Kannan, S.; James, A. J.; Sharp, P. R. *Polyhedron* **2000**, *19*, 155−163.

Table 1. Crystallographic and Data Collection Parameters for **2**, $Pd(OTf)_2$(dppma), and **7**[a]

	2	$Pd(OTf)_2$(dppma)	**7** (L_2 = dppip, X = OTF)	**7** (L_2 = dppma, X = OTF)
formula	$C_{25}H_{23}N_3O_6P_2Pt$	$C_{27}H_{23}F_6NO_6P_2PdS_2$	$C_{43}H_{44}F_6N_2O_6P_2PdS_2 \cdot CH_2Cl_2$	$C_{41}H_{41}F_6N_3O_6P_2PdS_2 \cdot 2C_7H_8$
fw	718.49	803.92	1116.19	1202.50
space group	$P\bar{1}$	$P1$	$P2_1/c$	$P2/n$
a, Å	11.091(3)	9.048(3)	12.678(2)	11.2832(11)
b, Å	14.376(3)	9.051(3)	12.1036(19)	12.4429(12)
c, Å	18.013(4)	11.395(3)	31.804(5)	20.1851(19)
α, deg	89.970(4)	97.873(5)	90	90
β, deg	77.020(4)	102.687(5)	91.659(3)	100.305(2)
γ, deg	73.632(4)	116.755(4)	90	90
V, Å^3	2679.3(10)	782.6(4)	4878.4(13)	2788.2(5)
Z	4	1	4	2
d_{calc}, g/cm^3	1.78	1.71	1.52	1.43
μ, mm^{-1}	5.40	0.906	0.712	0.536
R1,[b] wR2[c]	0.0767, 0.1940	0.0492, 0.1583	0.0476, 0.1029	0.0556, 0.1327

[a] λ = 0.710 70 Å (Mo), T = −100 °C. [b] $R1 = (\Sigma||F_o| - |F_c||)/\Sigma|F_o|$. [c] $wR2 = [(\Sigma w(F_o^2 - F_c^2)^2)/\Sigma w(F_c^2)^2]^{1/2}$.

Table 2. Crystallographic and Data Collection Parameters for **9**−**11**[a]

	9	**10** (M = Pt)	**10** (M = Pd)	**11** (M = Pt)	**11** (M = Pd)
formula	$C_{68}H_{70}BF_4LiN_4O_2P_4Pt_2 \cdot 3C_4H_{10}O_2$	$C_{74}H_{84}LiN_3P_4Pt_2Si_2 \cdot 4C_4H_8O$	$C_{74}H_{84}LiN_3P_4Pd_2Si_2 \cdot 4C_4H_8O$	$C_{66}H_{64}LiN_5O_3P_4Pt_2 \cdot C_4H_8O \cdot C_n$[d]	$C_{66}H_{64}LiN_5O_3P_4Pd_2 \cdot C_4H_8O \cdot C_n$[d]
fw	1853.45	1881.04	1703.66	1568.33[e]	1390.95[e]
space group	$P4/ncc$	$P\bar{1}$	$P\bar{1}$	$P2_1/m$	$P2_1/m$
a, Å	24.3639(18)	13.1670(17)	13.146(6)	11.4635(7)	11.5079(10)
b, Å	24.3639(18)	15.0144(19)	14.948(7)	24.1305(14)	24.026(2)
c, Å	28.208(3)	24.087(3)	24.173(12)	13.6535(8)	13.7686(12)
α, deg	90	89.121(2)	89.291(8)	90	90
β, deg	90	85.488(2)	85.350(8)	100.6360(10)	100.951(2)
γ, deg	90	67.937(2)	67.986(8)	90	90
V, Å^3	16744(2)	4398.9(10)	4388(4)	3711.9(4)	3737.5(6)
Z	8	2	2	2	2
d_{calc}, g/cm^3	1.470	1.420	1.289	1.403[e]	1.236[e]
μ, mm^{-1}	3.477	3.326	0.560	3.897[e]	0.612[e]
R1,[b] wR2[c]	0.0441, 0.0989	0.0315, 0.0728	0.0766, 0.1739	0.0401, 0.0781	0.0870, 0.1556

[a] λ = 0.710 70 Å (Mo), T = −100 °C. [b] $R1 = (\Sigma||F_o| - |F_c||)/\Sigma|F_o|$. [c] $wR2 = [(\Sigma w(F_o^2 - F_c^2)^2)/\Sigma w(F_c^2)^2]^{1/2}$. [d] C_n represents unresolved disordered solvent of crystallization. [e] Calculated without unresolved solvent of crystallization.

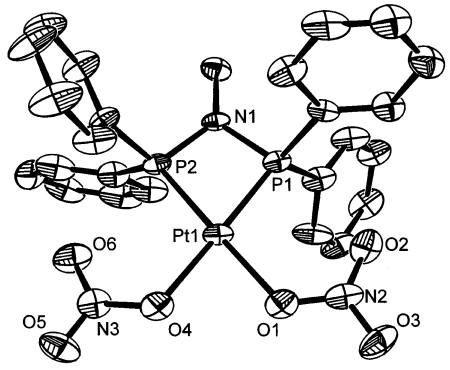

Figure 1. ORTEP drawing (50% probability ellipsoids) of one of two nearly identical independent molecules of $Pt(NO_3)_2$(dppma) (**2**).

Table 3. Selected Distances (Å) and Angles (deg) for $Pt(NO_3)$(dppma) (**2**)[a]

Pt1−P1	2.206(4)	Pt2−P3	2.200(3)
Pt1−P2	2.205(3)	Pt2−P4	2.216(3)
Pt1−O1	2.100(10)	Pt2−O7	2.096(8)
Pt1−O4	2.089(10)	Pt2−O10	2.078(9)
P2−Pt1−P1	72.41(13)	P3−Pt2−P4	72.28(13)
O4−Pt1−O1	76.4(4)	O10−Pt2−O7	76.0(3)

[a] Metrical parameters are given for both independent molecules.

for Pt demonstrating a reduced tendency to hydroxo formation in the Pd complexes. Treatment of $PdCl_2$(dppma) with AgX (X = OTf, BF_4) and water in CH_2Cl_2 yields, after workup, yellow products that give broad peaks in their ^{31}P NMR spectra. ^1H NMR spectra show dppma peaks and broad peaks attributed to OH or H_2O groups. Elemental analyses vary from sample to sample suggesting that these products are exchanging mixtures of complexes such as $[Pd(OH_2)_2(dppma)](X)_2$, $[Pd(OH_2)(X)(dppma)](X)$, $Pd(X)_2$(dppma), and $[Pd(\mu\text{-}OH)(dppma)]_2(X)_2$. Layering the CH_2Cl_2 reaction mixture (X = OTf) with Et_2O yields a small amount of crystals, which X-ray analysis shows to be $Pd(OTf)_2$(dppma).[9] A drawing of the complex is shown in Figure 2. An abbreviated summary of crystal data and data collection and processing is given in Table 1. Selected bond distances and angles are listed in Table 4.

An analogous reaction of $PdCl_2$(dppma) with $AgNO_3$ clearly gives a mixture of products. The ^{31}P NMR spectrum

(8) Other structurally characterized Pt(II) and Pd(II) nitrate phosphine complexes: (a) Countryman, R.; McDonald, W. S. *Acta Crystallogr., Sect. B* **1977**, *33*, 3580. (b) Jones, C. J.; McCleverty, J. A.; Rothin, A. S.; Adams, H.; Bailey, N. A. *J. Chem. Soc., Dalton Trans.* **1986**, 2055. (c) Suzuki, Y.; Miyamoto, T. K.; Ichida, H. *Acta Crystallogr., Sect. C* **1993**, *49*, 1318. (d) Gorla, F.; Togni, A.; Venanzi, L. M.; Albinati, A.; Lianza, F. *Organometallics* **1994**, *13*, 1607. (e) Rath, N. P.; Stockland, R. A., Jr.; Anderson, G. K. *Acta Crystallogr., Sect. C* **1999**, *55*, 494. (f) Redwine, K. D.; Wilson, W. L.; Moses, D. G.; Catalano, V. J.; Nelson, J. H. *Inorg. Chem.* **2000**, *39*, 3392. (g) Gul, N.; Nelson, J. H. *Organometallics* **2000**, *19*, 91. (h) Arendse, M. J.; Anderson, G. K.; Rath, N. P. *Acta Crystallogr., Sect. C* **2001**, *57*, 237. (i) Fernandez, D.; Sevillano, P.; Garcia-Seijo, M. I.; Castineiras, A.; Janosi, L.; Berente, Z.; Kollar, L.; Garcia-Fernandez, M. E. *Inorg. Chim. Acta* **2001**, *312*, 40.

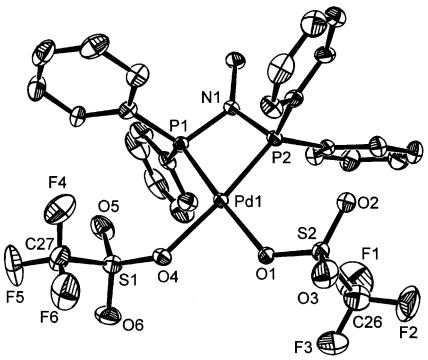

Figure 2. ORTEP drawing (50% probability ellipsoids) of $Pd(OTf)_2$(dppma).

Table 4. Selected Distances (Å) and Angles (deg) for $Pd(OTf)_2$(dppma)

Pd1−O1	2.134(8)	S1−O5	1.426(8)
Pd1−O4	2.146(7)	S1−O4	1.460(8)
Pd1−P2	2.222(2)	S2−O2	1.408(8)
Pd1−P1	2.228(3)	S2−O3	1.443(7)
S1−O6	1.416(8)	S2−O1	1.492(8)
O1−Pd1−O4	79.7(3)	O1−Pd1−P1	175.0(2)
O1−Pd1−P2	104.3(2)	O4−Pd1−P1	104.7(2)
O4−Pd1−P2	176.1(3)	P2−Pd1−P1	71.39(10)

of the reaction mixture and the isolated lemon yellow solid shows two sets of doublets at 32.7 and 26.5 ppm ($^2J_{P-P}$ = 21 Hz), and a singlet at 29.1 ppm. The two sets of doublets and the singlet observed in the ^{31}P NMR spectrum may be attributed to $[Pd(OH_2)(NO_3)(dppma)](NO_3)$ and $[Pd(NO_3)_2(dppma)]$, respectively. Presumably, observation of the individual peaks is due to slower exchange rates than for the OTf^- and BF_4^- derivatives as a result of stronger bonding of the nitrate ion to the Pd center. Conditions for isolating single products in these reactions are under investigation and will be reported separately. Meanwhile, these product mixtures, referred to as "$L_2Pd(X)_2$" (eq 3), are useful precursors for the preparation of mononuclear Pd diamine complexes (see below).

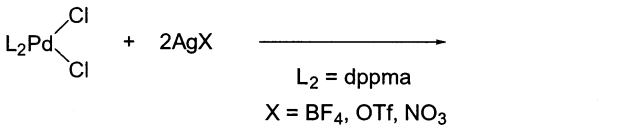

(3)

Unlike $PdCl_2$(dppma), $PdCl_2$(dppip) gives a single product when treated with AgOTf and small amounts of water in CH_2Cl_2. The pale yellow triflate-coordinated complex $Pd(OTf)_2$(dppip) (**3**) is isolated in 80% yield (eq 4) and gives satisfactory elemental analysis. The ^{31}P NMR spectrum of isolated **3** displays a single sharp peak at −16.5 ppm. The ^{1}H NMR spectrum shows peaks for the phosphine ligand but no OH peaks. The related complex $Pd(OTf)_2$(dppp)[9g] has been reported to readily exchange the triflate anions for water molecules under similar conditions.[10]

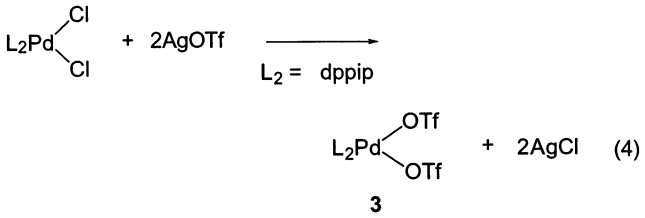

(4)

Platinum Amido and Amine Complexes. Reactions of aromatic amines with **1** and **2** produce bridged Pt diamido complexes or mononuclear diamine complexes depending on the Pt precursor, the amine, and the reaction conditions. The reaction of **1** (L_2 = dppma), with 4-toluidine at ambient temperature yields the diamido complex $[L_2Pt(\mu\text{-NHAr})]_2(BF_4)_2$ (**4**) (Ar = 4-tol, L_2 = dppma, eq 5). A similar reaction of **1** (L_2 = dppip) with aniline yields diamido complex **4** (Ar = Ph, L_2 = dppip), but with 4-toluidine, **4** (Ar = 4-tol, L_2 = dppip) is formed only upon refluxing the reaction mixture at 50 °C (eq 5).

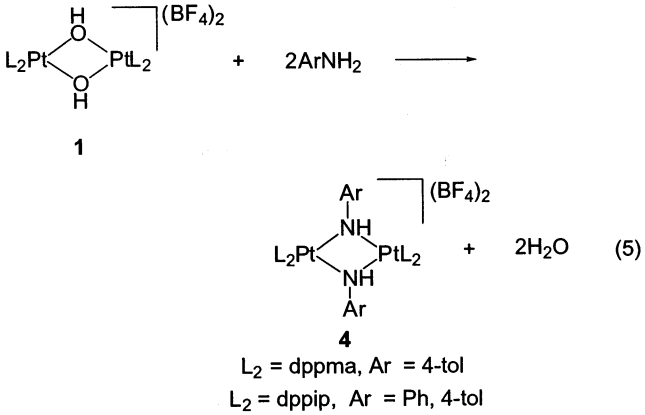

(5)

^{1}H NMR signals for the NH groups of **4** are observed as broad singlets or triplets between 4 and 5 ppm. These shifts are comparable to those observed for the dppm analogues but are at lower field than larger natural bite angle diphosphine analogues (dppe, dppp, dppb).[6] Like the dppm analogues, all 3 derivatives of **4** show evidence of hindered rotation about the N−Ar bond on the NMR time scale. In the absence of rotation, the *ortho* and *meta* hydrogen atoms of the aryl rings are all inequivalent and 4 peaks are expected. With rapid rotation the two *meta* hydrogen atoms become equivalent, the two *ortho* hydrogen atoms become equivalent, and only two peaks are expected. The dppip derivative with Ar = 4-tol shows two peaks at 50 °C (300 MHz) for the tol aromatic peaks. These two peaks are shifted upfield from

(9) Other structurally characterized Pt(II) and Pd(II) triflate phosphine complexes: (a) Appelt, A.; Ariaratnam, V.; Willis, A. C.; Wild, S. B. *Tetrahedron: Asymmetry* **1990**, *1*, 9−12. (b) Carr, N.; Mole, L.; Orpen, A. G.; Spencer, J. L. *J. Chem. Soc., Dalton Trans.* **1992**, 2653. (c) Bennett, B. L.; Birnbaum, J.; Roddick, D. M. *Polyhedron* **1995**, *14*, 187. (d) Bennett, B. L.; Birnbaum, J.; Roddick, D. M. *Polyhedron* **1995**, *14*, 187. (e) Aizawa, S.-I.; Yagu, T.; Kato, K.; Funahashi, S. *Anal. Sci.* **1995**, *11*, 557. (f) Stang, P. J.; Cao, D. H.; Saito, S.; Arif, A. M. *J. Am. Chem. Soc.* **1995**, *117*, 6273. (g) Stang, P. J.; Cao, D. H.; Poulter, G. T.; Arif, A. M. *Organometallics* **1995**, *14*, 1110−1114. (h) Sperrle, M.; Gramlich, V.; Consiglio, G. *Organometallics* **1996**, *15*, 5196−5201. (i) Vicente, J.; Arcas, A.; Bautista, D.; Jones, P. G. *Organometallics* **1997**, *16*, 2127. (j) Campora, J.; Lopez, J. A.; Palma, P.; Valerga, P.; Spillner, E.; Carmona, E. *Angew. Chem., Int. Ed.* **1999**, *38*, 147. (k) Annibale, G.; Bergamini, P.; Bertolasi, V.; Cattabriga, M.; Ferretti, V. *Inorg. Chem. Commun.* **2000**, *3*, 303. (l) Dahlenburg, L.; Mertel, S. *J. Organomet. Chem.* **2001**, *630*, 221. (m) Xia, A.; Sharp, P. R. *Polyhedron* **2002**, *21*, 1305−1310.

Chart 1

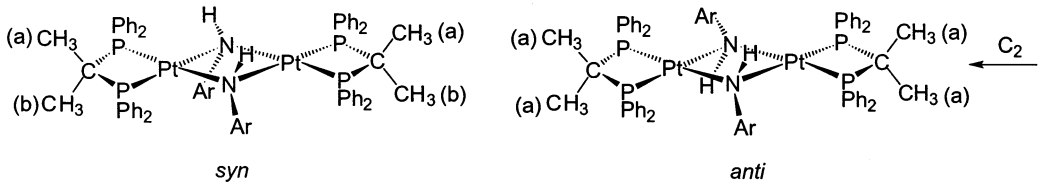

the usual aromatic region presumably by the "ring current" effect of "sandwiching" dppip phenyl rings. One is a sharp doublet at 5.71 ppm, and the other is a broad peak at 6.28 ppm. As the temperature is lowered, the broad peak becomes broader and reaches the coalescence point at 10 °C. Similarly, the sharp doublet becomes broader but does not reach the coalescence point until −10 °C. At −70 °C, 4 doublets are observed where the sharp doublet at 50 °C has resolved into two closely spaced doublets at 5.67 and 5.76 ppm and the broad peak at 50 °C has resolved into two widely spaced doublets at 5.36 and 6.36 ppm. This gives $\Delta G^{\ddagger}$ values for the rotation process of 53.8 and 55.4 kJ/mol for an average value of 55(1) kJ/mol.[11] Similar behavior is observed for the dppma derivative, and $\Delta G^{\ddagger}$ values of 58.9 and 61.9 kJ/mol (average value of 60(2) kJ/mol) are calculated. Detailed variable-temperature spectra were not recorded for the dppip Ph derivative. Comparison of spectra in $CDCl_3$ and CD_2Cl_2 indicate slower rotation rates in $CDCl_3$ than in CD_2Cl_2. This was also found for the dppm analogues.[6]

^{1}H NMR spectra of **4** also show signals for the dppip and dppma ligands. The phenyl groups are multiplets from 7.0 to 8.2 ppm, and the methyl groups are triplets ($^3J_{HP}$ = 15.0 and 12.5 Hz) at ca. 1 ppm (dppip) and just above 2 ppm (dppma). The dppip derivatives show two overlapping triplets for the methyl groups. This most likely indicates that **4**, at least for the dppip derivatives, has a syn orientation of the Ar groups (Chart 1) since this would give inequivalent dppip methyl groups. The alternate anti isomer has C_2 symmetry relating the two methyl groups, and only one triplet signal would be expected. The anti isomer could still give rise to two signals if the complex is folded at the shared N--N edge of the two square planar Pt centers. However, in general the energy difference between folded and planar structures is small in d^8 systems[12] and a static folded structure in solution is unlikely. Syn and anti isomers have been observed in solution with related systems.[6,13]

^{31}P NMR spectra for **4** show downfield shifts and smaller J_{Pt-P} values compared to the parent hydroxo complexes. The smaller J_{Pt-P} values are consistent with the greater donor strength of the amido ligands over the hydroxo ligand.[14]

With more sterically hindered 2,6-dimethylaniline, the reaction with **1** (L_2 = dppip) gives only the white mixed amido−hydroxo complex $[Pt_2(\mu\text{-OH})(\mu\text{-NHAr})(dppip)_2](BF_4)_2$ (**5**) (eq 6). No diamido complex is obtained even upon refluxing the reaction mixture with excess 2,6-dimethylaniline. The replacement of the second hydroxo group is presumably sterically inhibited as observed in related systems.[6]

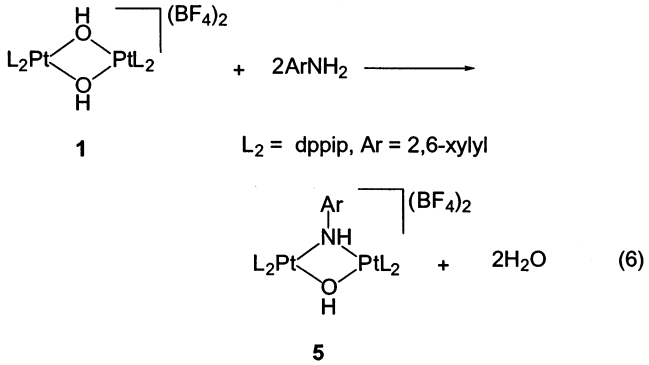

^{31}P NMR spectra of the amido−hydroxo complex **5** show two sets of doublets, one for the phosphorus trans to the OH group and one for the phosphorus trans to the NHAr group. The small P−P coupling of ∼60 Hz is consistent with a *cis*-phosphine geometry at the Pt centers.[14] Each phosphine doublet displays the expected ^{195}Pt satellites. The upfield doublet shows larger P−Pt coupling than the downfield doublet, and the coupling constant is similar to that of the starting hydroxo complex. Since coupling constants depend on the donor strength of the ligand trans to the phosphine atom, this signal is assigned to the phosphorus atom trans to the OH group.[14] The ^{1}H NMR spectrum of the complex shows two singlets at 2.34 and 4.61 ppm for the OH and NH groups. The amido ligand methyl groups resonate as two singlets at 3.32 and 1.64 ppm. The two *meta* protons resonate as doublets at 6.02 and 5.59 ppm, and the *para* proton resonates as a triplet at 5.95 ppm. The appearance of two signals for the amido methyl groups and the amido *meta* hydrogen atoms indicates the absence of rotation about the N−C bond of the amido ligand (on the NMR time scale). The dppip methyl groups are observed as two triplets (1.37 and 0.76 ppm) consistent with the low symmetry of the complex and the configuration at the nitrogen center.

(10) We assume that the indicated water addition of 2.0 and 10 mL in this report is in error and that the units should be μL and not mL.

(11) Lukehart, C. M. *Fundamental Transition Metal Organometallic Chemistry*; Brooks/Cole: Monterey, CA, 1985; p 200.

(12) (a) Summerville, R. H.; Hoffmann, R. *J. Am. Chem. Soc.* **1976**, *98*, 7240. (b) Aúllon, G.; Ujaque, G.; Lledós, A.; Alvarez, S.; Alemany, P. *Inorg. Chem.* **1998**, *37*, 804−813. (c) Aúllon, G.; Ujaque, G.; Lledós, A.; Alvarez, S. *Chem.—Eur. J.* **1999**, *5*, 1391−1410.

(13) (a) Brunet, J.-J.; Commenges, G.; Neibecker, D.; Philippot, K.; Rosenberg, L. *Inorg. Chem.* **1994**, *33*, 6373−6379. (b) Okeya, S.; Yoshimatsu, H.; Nakamura, Y.; Kawaguchi, S. *Bull. Chem. Soc. Jpn.* **1982**, *55*, 483−491. (c) Villanueva, L. A.; Abboud, K. A.; Boncella, J. A. *Organometallics* **1994**, *13*, 3921−3931. (d) Driver, M. S.; Hartwig, J. F. *J. Am. Chem. Soc.* **1996**, *118*, 4206−4207.

(14) (a) Pidcock, A.; Richards, R. E.; Venanzi, L. M. *J. Chem. Soc. A* **1966**, 1707−10. (b) Allen, F. H.; Pidcock, A. *J. Chem. Soc. A* **1968**, 2700. (c) Hartley, F. R. *The Chemistry of Platinum and Palladium*; Applied Science: Oxford, U.K., 1973. (d) Appleton, T. G.; Clark, H. C.; Manzer, L. E. *Coord. Chem. Rev.* **1973**, *10*, 335.

The mononuclear diamine complex $[L_2Pt(NH_2Ar)_2](NO_3)_2$ (**6**) (L_2 = dppma, Ar = 2,6-xylyl) is isolated from the reaction of $[L_2Pt(NO_3)_2]$ with 2,6-dimethylaniline (eq 7).

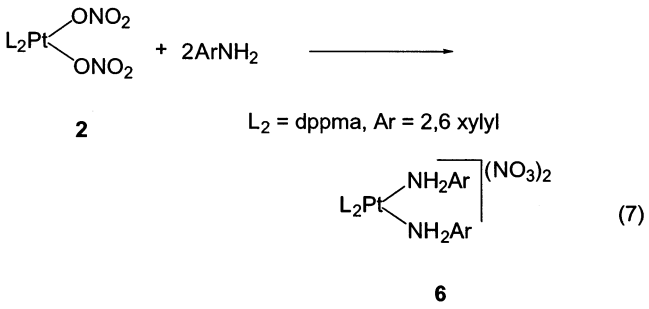

(7)

The ^{31}P NMR spectrum of the reaction mixture shows a broad peak at 13.6 ppm with J_{Pt-P} = 3222 Hz, whereas the isolated solid shows a sharp peak at 3.0 ppm with J_{Pt-P} = 3810 Hz. The small value of the Pt−P coupling constant (3222 Hz) for the reaction mixture suggests the presence of a strong-donor amido ligand trans to the P center.[14] The excess 2,6-dimethylaniline present in the reaction mixture is probably responsible for this behavior where reversible (broadness of the NMR signal) deprotonation of **6** by the aniline gives an amido ligand. However, precipitation must favor **6** and once **6** is isolated free from the excess 2,6-dimethylaniline there is no deprotonation. The ^1H NMR spectrum of isolated **6** shows peaks corresponding to the amine methyl groups (singlet at 2.16 ppm), the *meta* protons (doublet at 6.89 ppm), and the *para* protons (triplet at 6.59 ppm). The NH_2 signal is observed at 4.62 ppm.

Pd Amine Complexes. Addition of 4-toluidine to the mixtures "Pd(dppma)X_2" (X = BF_4, OTf) or the dppip triflate complex Pd(dppip)$(OTf)_2$ (**3**) yields the mononuclear Pd diamine complexes $[L_2Pd(NH_2\text{-}4\text{-}tol)_2](X)_2$ (**7**) (eq 8). ^1H NMR spectra of the complexes in $CDCl_3$ show NH_2 peaks at 5.85−6.28 ppm. ^{31}P NMR spectra show sharp singlets. The solid-state structures of **7** (L_2 = dppma, dppip; X = OTf) were determined by single-crystal X-ray diffraction.[15] Drawings of the structures, illustrating the hydrogen bonding of the OTf anions to the amine hydrogen atoms, are shown in Figure 3. Selected bond distances and angles are listed in Table 5. An abbreviated summary of crystal data and data collection and processing is given in Table 1.

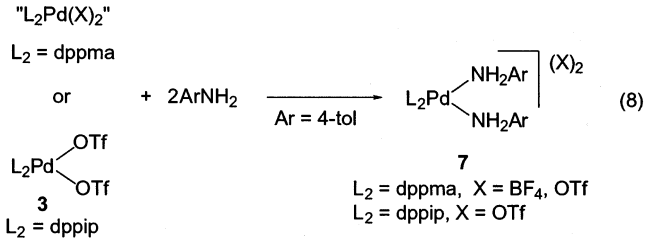

(8)

Similarly, addition of excess 2,6-dimethylaniline to "L_2-Pd$(NO_3)_2$" yields the mononuclear diamine Pd complex $[PdL_2(NH_2\text{-}2,6\text{-}xylyl)_2](NO_3)_2$ (**8**) (eq 9, L_2 = dppma). Unlike the analogous Pt complex **6**, the formation of an amido complex in the reaction mixture is not detected. The ^{31}P NMR spectrum of isolated diamine complex **8** and the reaction mixture are identical. The ^1H NMR spectrum of the diamine complex **8** shows the expected signals corresponding to the bidentate phosphine ligand and the coordinated amine with the NH_2 signal appearing at 3.62 ppm in CD_2Cl_2.

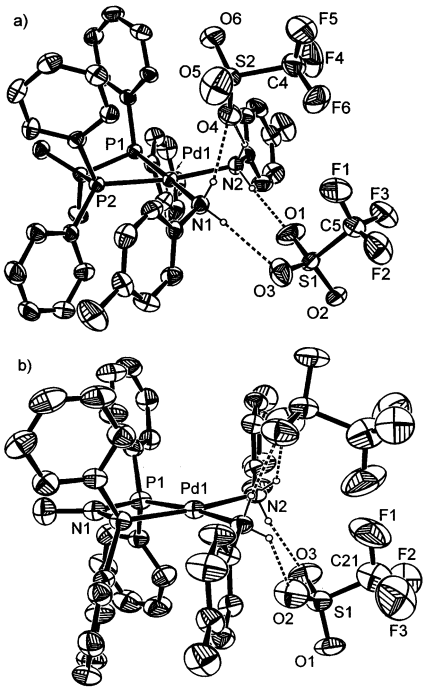

Figure 3. ORTEP drawings (50% probability ellipsoids) of $[Pd(NH_2\text{-}4\text{-}tol)_2L_2](OTf)_2$ (**7**) (L_2 = dppip (a), dppma (b); X = OTf). Labeled and unlabeled atoms in (b) are related by a 2-fold axis passing through Pd1 and N1.

Table 5. Selected Distances (Å) and Angles (deg) for $[Pd(NH_2\text{-}4\text{-}tol)_2L_2](OTf)_2$ (**7**) (L_2 = dppip, dppma; X = OTf)

	L_2 = dppip	L_2 = dppma
Pd1−N1	2.152(3)	
Pd1−N2	2.157(3)	2.135(4)
Pd1−P1	2.2596(9)	2.2478(16)
Pd1−P2	2.2671(9)	
N1−C51	1.447(4)	
N2−C61	1.440(4)	
N2−C14		1.450(7)
N1−Pd1−N2	83.56(11)	
N2−Pd1−N2		86.9(2)
P1−Pd1−P2	73.02(3)	
P1−Pd1−P1		71.51(8)

(15) Other structurally characterized Pt(II) and Pd(II) amine phosphine complexes: (a) Cooper, M. K.; Downes, J. M.; Goodwin, H. J.; McPartlin, M. *Inorg. Chim. Acta* **1983**, *76*, L157. (b) Park, S.; Hedden, D.; Rheingold, A. L.; Roundhill, D. M. *Organometallics* **1986**, *5*, 1305. (c) Miyamoto, T. K.; Matsuura, Y.; Okude, K.; Ichida, H.; Sasaki, Y. *J. Organomet. Chem.* **1989**, *373*, C8. (d) Matsuura, Y.; Okude, K.; Ichida, H.; Miyamoto, T. K.; Sasaki, Y. *Acta Crystallogr., Sect. C* **1992**, *48*, 357. (e) Suzuki, T.; Morikawa, A.; Kashiwabara, K. *Bull. Chem. Soc. Jpn.* **1996**, *69*, 2539. (f) Burrows, A. D.; Mingos, D. M. P.; Lawrence, S. E.; White, A. J. P.; Williams, D. J. *J. Chem. Soc., Dalton Trans.* **1997**, 1295. (g) van den Beuken, E. K.; Meetsma, A.; Kooijman, H.; Spek, A. L.; Feringa, B. L. *Inorg. Chim. Acta* **1997**, *264*, 171. (h) You, D.; Kim, E.; Kang, S. O.; Ko, J.; Lee, S. H. *Bull. Korean Chem. Soc.* **1998**, *19*, 565. (i) Habtemariam, A.; Watchman, B.; Potter, B. S.; Palmer, R.; Parsons, S.; Parkin, A.; Sadler, P. J. *J. Chem. Soc., Dalton Trans.* **2001**, 1306.

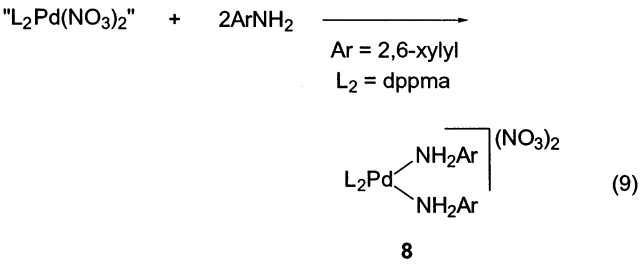

Pt and Pd Imido Complexes. As anticipated, a series of dinuclear diimido complexes is obtained by facile deprotonation of either the dimeric diamido complexes or the monomeric diamine complexes. Salts from the base are found to be associated with the imido complexes. The first of the series, yellow (M = Pt) or orange (M = Pd) **9** crystallize from a concentrated solution produced by adding excess LiN(SiMe$_3$)$_2$ to a DME suspension of the dppma Pt diamido complexes **4** or the dppma Pd amine complex **7** (eq 10). Spectroscopic and X-ray data indicate the isolation of a dimeric imido complex incorporating 1 equiv of Li(DME)X with the structure shown in eq 10.

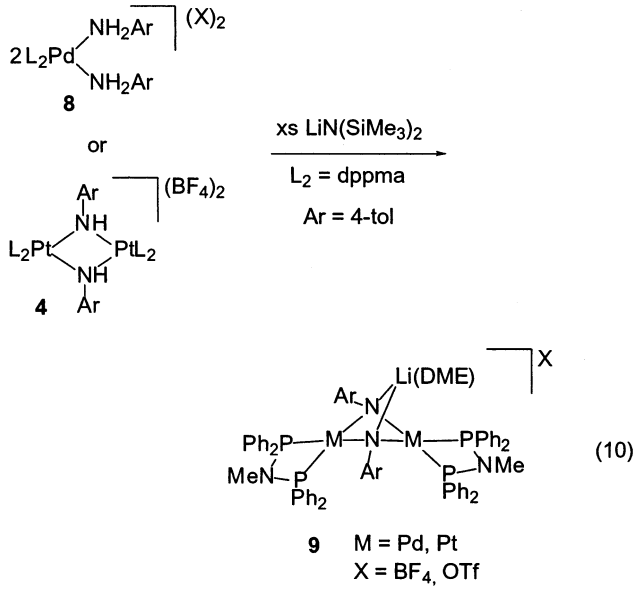

^{1}H NMR spectra of both the Pt and Pd derivatives of **9** in cold CD_2Cl_2 show signals for the chelated dppma ligands, the Li-coordinate DME, and the imido tol groups. The tol group *ortho* and *meta* protons appear as doublets indicating either facile rotation about the N−C bond or rapid exchange of the coordinated Li ion between the "top" and "bottom" faces of the [L$_2$Pt(μ-NAr)]$_2$ unit. ^{31}P NMR spectra of isolated **9** (M = Pt) show singlets within a range of 28−29 ppm flanked by ^{195}Pt satellites. The P−Pt coupling constants are reduced from those of the diamido complexes as expected for a stronger donor imido ligand.[14] Second-order coupling ($^2J_{Pt-P}$) of 81 Hz is observed in these complexes suggesting the presence of a Pt−Pt bond[14] and indicating integrity of the dimeric unit in solution. ^{31}P NMR spectra of **9** (M = Pd) show sharp singlets in a range 50−52 ppm. The structure of **9** (M = Pt, X = BF_4) was determined by single-crystal X-ray diffraction. A drawing of the cationic portion is shown in Figure 4. An abbreviated summary of crystal data and data collection and processing is given in Table 2. Selected bond distances and angles are listed in Table 6. The structure reveals the expected interaction of the DME-coordinated Li cation with the bridging imido group nitrogen atoms.

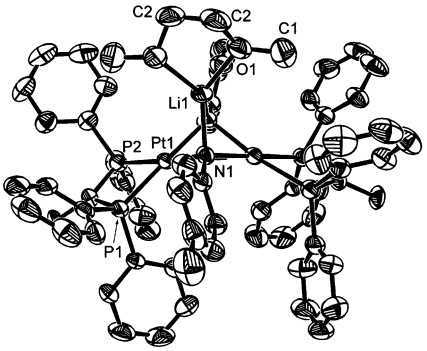

Figure 4. ORTEP drawing (50% probability ellipsoids) of [{Pt(μ-N-4-tol)(dppma)}$_2$·Li(DME)](BF$_4$) (**9**) (M = Pt; Ar = 4-tol). Labeled and unlabeled atoms are related by 2-fold axis bisecting the C2−C2 bond and passing through the Li atom.

Table 6. Selected Distances (Å) and Angles (deg) for [{Pt(μ-N-4-tol)(dppma)}$_2$·Li(DME)](BF$_4$) (**9**) (M = Pt; Ar = 4-tol)

Pt1−N1	2.061(6)	Pt1−Pt1	2.8519(6)
Pt1−N1	2.062(6)	Li1−O1	1.988(16)
Pt1−P1	2.235(2)	Li1−N1	2.032(16)
Pt1−P2	2.242(2)	N1−C4	1.395(10)
Pt1−Li1	2.827(17)	C2−C2	1.49(2)
N1−Pt1−N1	73.7(3)	P1−Pt1−P2	71.41(8)
N1−Pt1−P1	178.34(18)	C2−O1−C1	112.9(9)
N1−Pt1−P1	105.57(18)	C2−O1−Li1	109.4(7)
N1−Pt1−P2	109.49(18)	C1−O1−Li1	124.2(8)
N1−Pt1−P2	172.02(18)	O1−Li1−O1	82.7(8)

A similar reaction of the dppip Pt diamido dimers **4** or the dppip Pd diamine complex **7** with LiN(SiMe$_3$)$_2$ in THF or DME yields pale yellow Pt or red Pd imido complexes **10** (eq 11). As with the dppma imido complexes **9**, a Li ion is associated with **10**; however, for **10** it is the ion pair LiN(SiMe$_3$)$_2$ and not Li(DME)$^+$ that coordinates to the bridging imido groups.

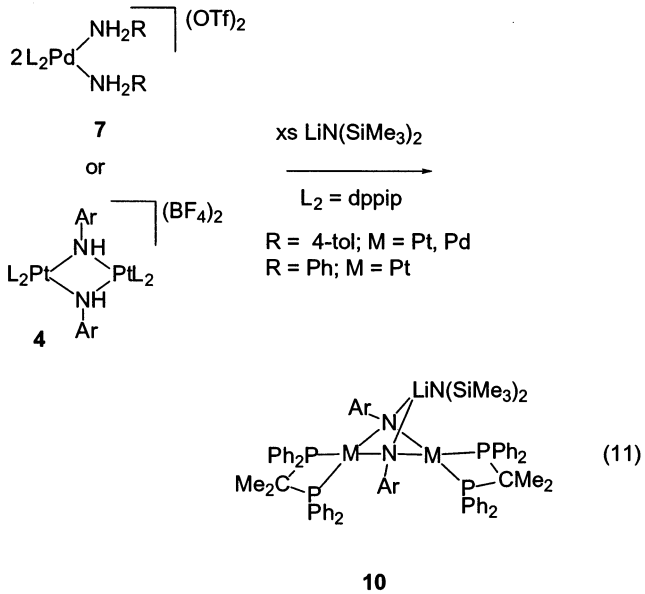

Table 7. Selected Distances (Å) and Angles (deg) for [M(μ-N-4-tol)(dppip)]$_2$·LiN(SiMe$_3$)$_2$ (**10**) (M = Pt, Pd; Ar = 4-tol)

	M = Pt	M = Pd		M = Pt	M = Pd
M1−M2	2.8615(3)	2.7920(12)	M2−N2	2.062(4)	2.076(5)
M1−P2	2.2506(12)	2.288(2)	N1−C1N	1.412(6)	1.387(9)
M1−P1	2.2516(12)	2.286(2)	N2−C8N	1.411(6)	1.411(8)
M2−P3	2.2487(13)	2.285(2)	Li1−N1	2.052(9)	2.008(15)
M2−P4	2.2670(12)	2.319(2)	Li1−N2	2.050(9)	2.011(14)
M1−N1	2.065(4)	2.069(5)	Li1−N3	1.963(9)	1.980(15)
M1−N2	2.059(3)	2.051(5)	M1−Li1	2.827(7)	2.794(13)
M2−N1	2.056(4)	2.061(6)	M2−Li1	2.880(8)	2.826(13)
P2−M1−P1	73.84(4)	73.86(7)	C1N−N1−M2	123.1(3)	122.9(4)
P3−M2−P4	73.48(5)	73.19(7)	C8N−N2−M1	124.7(3)	124.7(4)
N1−M1−N2	73.23(14)	74.7(2)	C8N−N2−M2	120.7(3)	119.3(4)
N1−M2−N2	73.37(15)	74.4(2)	Li1−N1−M1	86.7(3)	86.5(4)
M1−N1−M2	87.98(15)	85.1(2)	Li1−N1−M2	89.0(3)	88.0(4)
M1−N2−M2	87.95(14)	85.16(18)	Li1−N2−M1	86.9(3)	86.9(4)
C8N−N2−Li1	134.2(4)	137.6(6)	Li1−N2−M2	88.9(3)	87.5(4)
C1N−N1−M1	128.6(3)	128.7(4)			

^{1}H NMR spectra of **10** (M = Pt, Pd) show the SiMe$_3$ group of the coordinated Li(NSiMe$_3$)$_2$ as a singlet at 0.05 ppm. Consistent with the solid-state structure, the dppip methyl groups are observed as two triplets indicating inequivalence of the "top" and "bottom" methyl groups and suggesting that dissociation of the coordinated Li(NSiMe$_3$)$_2$ and/or inversion at the imido nitrogen center is slow on the NMR time scale. As with the Li(DME)X adducts **9**, the imido aryl groups of **10** show equivalence of the *ortho* and *meta* protons. In these complexes, the equivalence must come about by free rotation about the C−N bond as other exchange processes (e.g. dissociation of coordinated Li(NSiMe$_3$)$_2$) would also exchange the dppip methyl groups. ^{31}P NMR spectra of **10** (M = Pt) show singlets at −12.8 ppm with satellites ($^1J_{Pt-P}$ = 2758 Hz) and second-order P−Pt coupling of 60 Hz for both Ph and 4-tol derivatives. The Pd imido complex **10** (M = Pd) shows a singlet at 8.9 ppm. The $^1J_{Pt-P}$ coupling constants in the Pt imido complexes are lower than the starting diamido/amine complexes, consistent with the stronger donor strength of imido over amine and amido ligands.[14]

The molecular structures of both Pt and Pd diimido complexes **10** (R = 4-tol) were determined by single-crystal X-ray diffraction. Crystals of the Pt and Pd derivatives are isomorphous and isostructural. A drawing of the Pd structure, essentially identical with that of the Pt derivative, is given in Figure 5 and shows the interaction of the Li(NSiMe$_3$)$_2$ with the imido nitrogen atoms. An abbreviated summary of crystal data and data collection and processing for both structures is given in Table 2. Selected bond distances and angles are listed in Table 7.

Spectroscopic data indicate that dppip Pt and Pd diimido complexes are also isolated when NaN(SiMe$_3$)$_2$ is used as the base but without NaN(SiMe$_3$)$_2$ coordination to the bridged imido groups. (No SiMe$_3$ signals are detected by ^{1}H NMR.) A signal at −79 or −156 ppm in the ^{19}F NMR spectra indicates the presence of NaOTf or NaBF$_4$ in these imido complexes probably bridging the imido nitrogen atoms through the Na ion as observed for LiN(SiMe$_3$)$_2$ in **10** and LiNO$_3$ in **11** (see below).

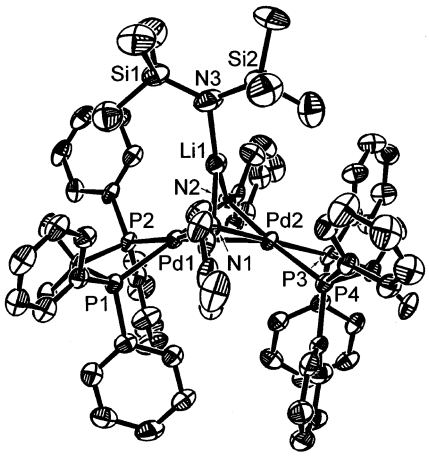

Figure 5. ORTEP drawing (50% probability ellipsoids) of [Pd(μ-N-4-tol)(dppip)]$_2$·LiN(SiMe$_3$)$_2$ (**10**) (M = Pd, Ar = 4-tol).

Ion pair association is also observed when the dppma Pt and Pd amine complexes **6** and **8**, with nitrate counterions,are deprotonated. Treatment of these complexes with excess LiN(SiMe$_3$)$_2$ gives the diimido complexes **11**, which are associated with LiNO$_3$ (eq 12). The ^{31}P NMR spectra of these complexes are similar to the dppma imido complexes **9**. However, no second-order P−Pt coupling is observed in the Pt derivatives. This is consistent with the relatively long Pt−Pt distance (3.1034(4) Å) observed in the X-ray crystal structure. The ^{1}H NMR spectrum of the Pt derivative shows equivalent xylyl *meta* hydrogen atoms and *ortho* methyl groups. In this case, the equivalence could be either from free rotation about the N−C bond or from rapid exchange of LiNO$_3$ between the "top" and "bottom" face of [L$_2$Pt(μ-NAr)]$_2$. The Pd derivative is very reactive with solvents, and ^{1}H NMR data could not be obtained. Single-crystal X-ray data for both the Pt and Pd derivatives show that their crystals are isomorphous and that the complexes are isostructural. A drawing of the Pd structure, essentially identical to that of the Pt derivative, is given in Figure 6 and shows the interaction of the LiNO$_3$ with the imido nitrogen atoms. An abbreviated summary of crystal data and data collection and processing for both structures is given in Table 2. Selected

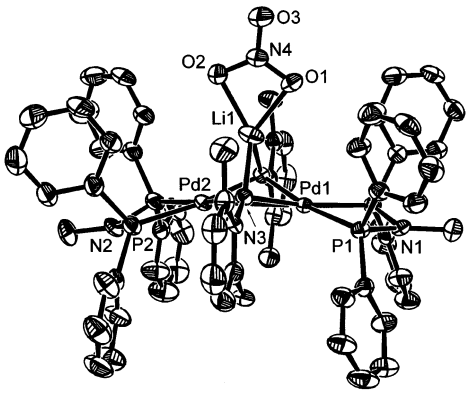

Figure 6. ORTEP drawing (50% probability ellipsoids) of [Pd(μ-N-2,6-xylyl)(dppma)]$_2$·$LiNO_3$ (**11**) (M = Pd). Labeled and unlabeled atoms are related by a mirror plane containing the Pd and Li atoms.

bond distances and angles are listed in Table 8.

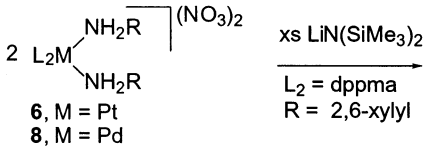

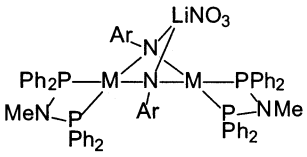

(12)

11

Deprotonation of [(L_2Pt)$_2$(μ-NHAr)(μ-OH)](BF$_4$)$_2$ (L_2 = dppip). Addition of excess LiN(SiMe$_3$)$_2$ to a white suspension of the amido−hydroxo complex **5** in THF forms a pale yellow homogeneous solution containing the doubly deprotonated oxo−imido complex **12**, which is associated (by NMR) with both $LiBF_4$ and LiN(SiMe$_3$)$_2$ (eq 13).

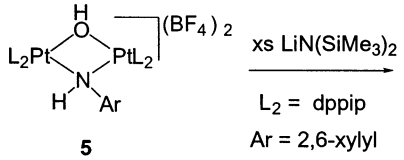

5

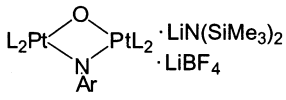

(13)

12

^{31}P NMR spectra of the reaction mixture and isolated **12** show a pair of doublets (J_{P-P} = 40 Hz) flanked by ^{195}Pt satellites with coupling constants lower than the starting amido−hydroxo complex **5**. The upfield doublet shows a larger coupling constant than the downfield doublet similar in magnitude to that observed for the Pt dioxo complex **13** (see below). In contrast to the diimido complexes **9** and **10** but in common with the dioxo complex **13** and the diimido complex **11**, second-order P−Pt coupling is not observed in the ^{31}P NMR spectrum of **12**. The ^{1}H NMR spectrum of isolated **12** shows signals for the dppip ligand and the imido group. No NH or OH signals are observed. The dppip methyl groups are inequivalent and are observed as two triplets indicating a structure with a different "top" and "bottom" face. The methyl groups of the imido 2,6-xylyl ligand resonate as a broad singlet at 2.1 ppm, the two *meta* protons resonate at 6.5 ppm as a broad doublet, and the *para* proton resonates as a triplet at 6.2 ppm. The appearance of a broad singlet for the xylyl methyl groups and the *ortho* and *meta* hydrogen atoms suggests hindered rotation about the N−C bond but less so than in the parent amido−hydroxo complex **5**, which gives separate signals for each of the methyl groups and hydrogen atoms. The presence of LiN(SiMe$_3$)$_2$ in the isolated complex is indicated by the observation of the $SiMe_3$ group as a singlet at 0.05 ppm. The ^{19}F NMR spectrum shows a peak at −154 ppm indicating the presence of the BF_4 anion and the incorporation of $LiBF_4$.

Deprotonation of [L_2Pt(μ-OH)$_2$](BF$_4$)$_2$ (L_2 = dppip). Addition of excess LiN(SiMe$_3$)$_2$ to dihydroxo dimer **1** in THF forms the dioxo complex **13** where associated LiN(SiMe$_3$)$_2$ and $LiBF_4$ units are probably coordinated to the oxo ligands (eq 14). The reaction bears similarity to the above imido preparations and to previous dioxo preparations for other phosphine ligand complexes of Pt.[5,6]

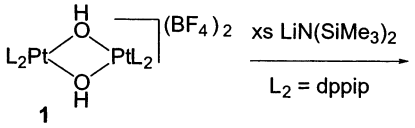

1

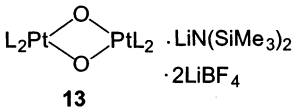

(14)

13

The ^{31}P NMR spectra of the isolated complex and the reaction mixture show a broad peak with ^{195}Pt satellites. The coupling constant is 100 Hz lower than the hydroxo precursor as anticipated for the stronger trans-donor oxo ligand. The ^{1}H NMR spectrum of **13** shows only one dppip methyl group triplet suggesting a more symmetric structure than that found for the imido analogues **10** or rapid (on the NMR time scale) dissociation of Li ions in solution. The $SiMe_3$ group signal is found at 0.05 ppm. Analytical data indicate the presence of one LiN(SiMe$_3$)$_2$, but ^{1}H NMR data on different samples show this can vary between 1 and 2.

^{31}P NMR spectra of the reaction mixtures when NaN(SiMe$_3$)$_2$ and KN(SiMe$_3$)$_2$ are used as deprotonating bases show a singlet with satellites, shifted by ∼2 ppm relative to that of **13**. Pt−P coupling constants are 50 Hz smaller than **13** suggesting a stronger oxo donor. ^{1}H NMR spectra of the isolated solids show no signals for $SiMe_3$ groups. However, ^{19}F NMR spectra show signals at −156 ppm indicating the presence of BF_4^- and the likely presence of MBF_4 (M = Na, K). Although not fully characterized, these complexes are probably analogues of **13** but with MBF_4 association instead of LiN(SiMe$_3$)$_2$. A stronger donor oxo ligand in these complexes would be expected given the weaker M−oxo interaction with the large Na^+ and K^+ ions as opposed to the small, high charge density Li^+ ions of **13**.

Table 8. Selected Distances (Å) and Angles (deg) for [M(μ-N-2,6-xylyl)(dppma)]$_2$·LiNO$_3$ (**11**) (M = Pt, Pd)

	M = Pt	M = Pd		M = Pt	M = Pd
M1−M2	3.1034(4)	3.0146(10)	Li1−M2	2.687(13)	2.652(16)
M1−P1	2.2521(13)	2.2856(17)	Li1−O1	2.023(14)	2.040(17)
M2−P2	2.2511(14)	2.2876(19)	Li1−O2	2.080(13)	2.060(18)
M1−N3	2.062(4)	2.053(5)	Li1−N3	2.080(10)	2.041(14)
M2−N3	2.055(4)	2.062(5)	N3−C3	1.426(6)	1.401(8)
Li1−M1	2.670(11)	2.651(18)			
P1−M1−P1	71.04(6)	70.90(9)	N3−M2−N3	74.8(2)	76.2(3)
P2−M2−P2	70.68(8)	70.82(10)	C3−N3−M2	119.9(3)	118.8(4)
N3−M1−P1	172.64(11)	170.60(14)	C3−N3−M1	120.9(3)	120.3(4)
N3−M2−P2	173.91(11)	172.30(15)	M2−N3−M1	97.83(16)	94.2(2)
N3−M1−P1	106.75(11)	105.54(14)	C3−N3−Li1	143.9(4)	147.4(5)
N3−M2−P2	106.94(11)	106.02(14)	M2−N3−Li1	81.1(3)	80.6(4)
N3−M1−N3	74.5(2)	76.6(3)	M1−N3−Li1	80.3(3)	80.7(5)

Discussion

As described in the Introduction, this work was initiated to test the concept that small natural bite angle diphosphine ligands favor the deprotonation of amido groups in the dimeric Pt(II) complexes $[L_2Pt(NHAr)]_2^{n+}$. This concept originated from our previous observations on the $L_2 = Ph_2P(CH_2)_xPPh_2$ ($x = 1-4$) ligand system, where only the $n = 1$ (dppm) ligand complexes can be deprotonated[6] but only after the dppm methylene group is deprotonated (Scheme 1) making an unambiguous conclusion on a bite angle effect difficult. The ligands, dppip and dppma, used in the present work do not contain an acidic hydrogen but have a similarly small natural bite angle, and indeed the diamido and amine complexes derived from them are readily deprotonated to yield imido complexes. The origin of this enhanced acidity for the small natural bite angle diphosphine complexes could be either kinetic or thermodynamic. We have begun pK_a studies in a closely related amido−hydroxo system, and initial results indicate that the thermodynamic acidity of the dppip complex is actually slightly less than that of the analogous dppe complex.[16] Thus, in the current diamido systems it is likely that the enhanced acidity is kinetic. That is, the larger natural bite angle diphosphine complexes studied earlier should deprotonate but the reaction is too slow to be observed. The inhibition is probably steric in origin where the phenyl groups of the diphosphine ligand prevent approach of the base to the amido ligands. With the small bite angle diphosphine ligands the phenyl groups are held further away from the amido ligands allowing base access. This suggests that diamido complexes prepared with larger natural bite angle diphosphine ligands with the phenyl groups replaced by smaller groups (e.g. Me, Et) will be readily deprotonated.

A second aspect of the small bite angle of the diphosphine ligands, important in our successful Pd diimido syntheses, is their ability to stabilize Pt(II) and Pd(II) centers to reduction as observed in decreases in reductive elimination rates of Ni(II),[17] Pd(II),[18] and Pt(II)[19] complexes with decreasing diphosphine bite angle and in the reversibility of dioxygen coordination to M^0 (M = Ni, Pd, Pt) complexes.[20] In our previous attempts to prepare Pd analogues of Pt imido and oxo complexes by deprotonation, the precipitation of Pd metal was observed on base addition. This is consistent with the greater ease of reduction of Pd over Pt allowing electron-transfer pathways to dominate. With the small bite angle diphosphine ligands dppma and dppip, the reduction pathway is suppressed allowing deprotonation to dominate.

As shown by Figures 2−4 and by the spectroscopic data, the imido complexes are all found to be associated with Li or Na ions. This is an indication of the basicity of the imido ligands in these complexes and is consistent with the expected lack of interaction of the imido nitrogen lone pair with the metal centers. In addition, the geometry of the Pt_2N_2 unit ideally orients the lone pairs allowing the unit to act as a chelating $4e^-$ donor for the metal cations. Although we do not believe these interaction are needed for the formation of the complexes, they undoubtedly do add to their stability.

All of the imido complexes were prepared using similar reaction conditions with a large excess of $LiN(SiMe_3)_2$. The different Li salts, $LiNO_3$, Li(DME)X, or $LiN(SiMe_3)_2$, associated with the isolated complex appear to be the result of solubility differences with the least soluble crystallizing from the reaction mixture. This is suggested by the synthesis of the $LiNO_3$ adduct **11**. If the deprotonation reaction is conducted with a slight excess of $LiN(SiMe_3)_2$ the same $LiNO_3$ adduct **11** is isolated but it precipitates from the reaction mixture as a microcrystalline solid. This solid redissolves on addition of excess $LiN(SiMe_3)_2$, and the $LiNO_3$ adduct may then be slowly precipitated as a crystalline solid by cooling the solution. Similarly, the $Li(DME)^+$ adduct **9** dissolves readily in DME only if $LiN(SiMe_3)_2$ is present and reprecipitates as a crystalline solid on cooling the solution. These observations suggest solution equilibria of the type shown in eq 15, where the $LiN(SiMe_3)_2$ adduct is more soluble than the $LiNO_3$ adduct. Other possible equilibria are evidenced by the isolation of the Li(DME)X adducts **9,** where solvent coordination to the Li ion has disrupted the ion paring observed in **10** and **11**. This undoubtedly happens in all of

(16) Anandhi, U.; Sharp, P. Work in progress.

(17) Kohara, T.; Yamamoto, T.; Yamamoto, A. *J. Organomet. Chem.* **1980**, *192*, 265.
(18) Marcone, J. E.; Moloy, K. G. *J. Am. Chem. Soc.* **1998**, *120*, 8527−8528.
(19) Hofmann, P.; Heiss, H.; Neiteler, P.; Muller, G.; Lachmann, J. *Angew. Chem.* **1990**, *102* (8), 935−938; *Angew. Chem., Intl. Ed. Engl.* **1990**, *29*, 880.
(20) Yoshida, T.; Tatsumi, K.; Otsuka, S. *Pure Appl. Chem.* **1980**, *52*, 713−727.

the solutions with again the least soluble form being isolated as the solid. Similar arguments can be applied to the oxo−imido and the dioxo complexes. However, the much less sterically demanding oxo ligand allows interaction of more than a single salt.

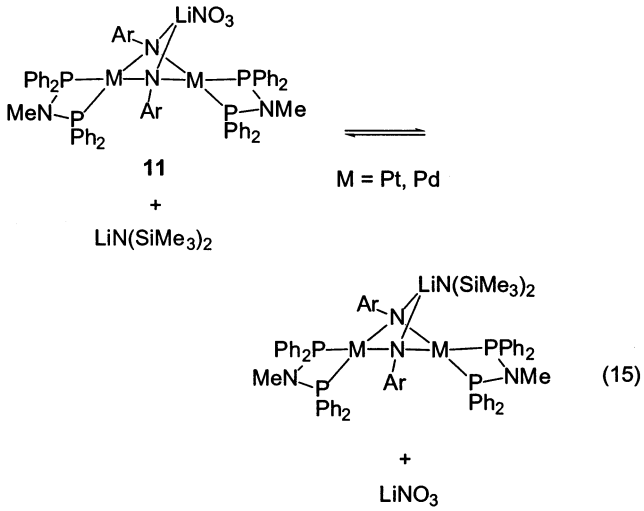

(15)

The structures of **9**−**11** confirm their identity as dimeric bridging imido complexes with Li ion bonding to the imido group nitrogen atoms. Also confirmed is the short Pt−Pt distance in complexes **9** (2.8519(6) Å) and **10** (2.8615(3) Å) indicated by the observation of second-order P−Pt coupling in these two complexes. The longer distance in **11** (3.1034(3) Å) is also indicated by the absence of second-order P−Pt coupling. The short distance in **9** and **10** is achieved by folding of the structures at the common N−N edge of the two square planar metal centers (**9**, 58°; **10**, 57° (Pt), 59° (Pd)). The longer M−M distance of **11** results from a smaller fold angle (Pt, 28°; Pd, 32°) that keeps the two metal centers apart. The small fold angle of **11** may be attributed to steric effects of the xylyl methyl groups. The observed second-order P−Pt coupling in the Pt derivatives of **9** and **10** also indicates that the dimeric structures are retained in solution. Thus, there is no indication of the monomeric form $L_2Pt{=}NAr$ recently reported for the Ni imido complex $L_2Ni{=}NAr$.[21]

A shortening of the M−N distances in the imido complexes from those of the precursor amido and amine complexes is expected given the greater donor strength of the imido ligand. The average M−N bond distances for the imido complexes are 2.062(1), 2.060(4), and 2.058(5) Å for Pt and 2.06(6) and 2.058(6) Å for Pd with all falling in a tight range around 2.06 Å. This is clearly shorter than the Pd amine complexes **7**, which have an average Pd−N distance of 2.15(1) Å. While there are no structures for amido complexes with dppma and dppip ligands, those reported in the literature with other phosphine ligands trans to bridging amido groups have average Pt−N or Pd−N distances that range from 2.082(4) to 2.15(3)[6,9m,22] again demonstrating shorter distances for the imido complexes reported here.

(21) Mindiola, D. J.; Hillhouse, G. L. *J. Am. Chem. Soc.* **2001**, *123*, 4623−4624.

Conclusions

The small natural bite angle diphosphines, $Ph_2PN(Me)PPh_2$ (dppma) and $Ph_2PC(Me_2)PPh_2$ (dppip), enhance the acidity of the Pt(II) and Pd(II) arylamine and arylamido complexes $[L_2M(NH_2Ar)]^{2+}$ and $[\{L_2Pt(\mu\text{-}NHAr)\}_2]^{2+}$ over those of analogous larger natural bite angle diphosphine complexes. The acidity enhancement is probably kinetic and results from reduced steric crowding of the nitrogen centers by the Ph_2P units. This bite angle effect, along with a likely reductive stabilization, has allowed the preparation of the Pt and Pd imido complexes, $[\{L_2M(\mu\text{-}NAr)\}_2]$ (M = Pt, Pd), by deprotonation. The imido complexes are isolated, and probably also exist in solution, as complexes with the Li, Na, or K ion from the base $LiN(SiMe_3)_2$, $NaN(SiMe_3)_2$, or $KN(SiMe_3)_2$ by coordination to the ion through the imido nitrogen atoms.

Experimental Section

General Procedures. Experiments were performed under a dinitrogen atmosphere in a Vacuum Atmospheres Corporation drybox. Solvents were dried by standard techniques and stored under dinitrogen over 4 Å molecular sieves or sodium metal. The ligands dppip[23] and dppma[24] and the metal complexes L_2PtCl_2 and L_2PdCl_2 (L_2 = dppip,[25] dppma[26]) were synthesized by literature procedures. Silver salts and amines were purchased from commercial sources and used as received. NMR spectra were recorded on a Bruker AMX-250 spectrometer at 25 °C. Shifts are given in ppm with positive values downfield of TMS (^1H), external H_3PO_4 (^{31}P), or $CFCl_3$ (^{19}F). Desert Analytics or Atlantic Micro Lab or National Chemical Consulting performed the microanalyses (inert atmosphere). The presence of CH_2Cl_2 of crystallization in the analyzed samples was confirmed by ^1H NMR spectroscopy in $CDCl_3$.

Platinum Complexes. $[L_2Pt(\mu\text{-}OH)]_2(BF_4)_2$ (1) (L_2 = dppip, dppma). To a stirred CH_2Cl_2 (10 mL) suspension of L_2PtCl_2 (0.226 mmol) is added solid $AgBF_4$ (0.092 g, 0.47 mmol) in portions. The mixture is stirred for 1 h in the dark, after which time the AgCl precipitate is filtered off with the aid of diatomaceous earth. The clear filtrate is concentrated under reduced pressure, and the white product is precipitated with diethyl ether. Yield: 68−70% (∼100 mg). Samples for analysis were obtained by recrystallization from CH_2Cl_2/Et_2O. dppip: $^{31}P\{^1H\}$ NMR (CH_2Cl_2) −30.5 (s with satellites, J_{Pt-P} = 3125 Hz); ^1H NMR (CD_2Cl_2) 8.24−7.55 (m, 40H, Ph), 2.02 (br s, OH), 1.37 (t, $^3J_{P-H}$ = 15.0 Hz, 12H, CMe_2). Anal. Calcd (found) for $C_{54}H_{54}B_2F_8O_2P_4Pt_2{\cdot}0.5CH_2Cl_2$: C, 44.65 (44.96); H, 3.79 (3.97). dppma: $^{31}P\{^1H\}$ NMR (CH_2Cl_2) 10.5 (s with

(22) (a) O'Mahoney, C. A.; Parkin, I. P.; Williams, D. J.; Woollins, J. D. *Polyhedron* **1989**, *8*, 1979−1981. (b) Park, S.; Rheingold, A. L.; Roundhill, D. M. *Organometallics* **1991**, *10*, 615−623. (c) Alcock, N. W.; Bergamini, P.; Kemp, T. J.; Pringle, P. G.; Sostero, S.; Traverso, O. *Inorg. Chem.* **1991**, *30*, 1594−1598. (d) Villanueva, L. A.; Abboud, K. A.; Boncella, J. M. *Organometallics* **1994**, *13*, 3921−3931. (e) Xu, X.; James, S. L.; Mingos, D. M. P.; White, A. J. P.; Williams, D. J. *J. Chem. Soc., Dalton Trans.* **2000**, 3783−3790. (f) Xia, A.; Sharp, P. *Inorg. Chem.* **2001**, *40*, 4016−4021.

(23) Hewertson, W.; Watson, N. R. *J. Chem. Soc.* **1962**, 1490−93.

(24) (a) Ewart, G.; Lane, A. P.; McKechnie, J.; Payne, D. S. *J. Chem. Soc.* **1964**, 1543−1547. (b) Wang, F. T.; Najdzionek, J.; Leneker, K. L.; Wasserman, H. B. D. M. *Synth. React. Inorg. Metal-Org. Chem.* **1978**, *8*, 119. (c) Sekabunga, E. J.; Smith, M. L.; Webb, T. R.; Hill, W. E. *Inorg. Chem.* **2002**, *41*, 1205−1214.

(25) Barkley, J.; Ellis, M.; Higgins, S. J.; McCart, M. K. *Organometallics* **1998**, *17*, 1725−1729.

(26) Browning, C. S.; Farrar, D. H. *J. Chem. Soc., Dalton Trans.* **1995**, 521−530.

satellites, $J_{Pt-P} = 3483$ Hz); ^{1}H NMR (CD_2Cl_2) 7.73−7.58 (m, 40H, Ph), 3.02 (br s, OH) 2.50 (t, $^3J_{P-H} = 12.5$ Hz, 6H, N−Me). Within minutes of dissolution, the ^{1}H and ^{31}P NMR spectra of the dppma complex indicate the presence of a small quantity of an unidentified complex (^{31}P peak at 9.3). However, the purity of the isolated product is confirmed by elemental analysis. Anal. Calcd (found) for $C_{50}H_{48}B_2F_8N_2O_2P_4Pt_2$: C, 42.97 (42.62); H, 3.47 (3.56); N, 2.01 (2.01).

[Pt(NO$_3$)$_2$(dppma)] (2). To a stirred suspension of (dppma)-$PtCl_2$ (0.100 g, 0.150 mmol) in 10 mL of CH_2Cl_2 is added solid $AgNO_3$ (0.150 g, 0.883 mmol) in portions. The mixture is stirred for 3 h. The AgCl precipitate and excess $AgNO_3$ are then removed by filtration through a pad of diatomaceous earth. The resulting clear filtrate is concentrated under reduced pressure, and the analytically pure white product is precipitated with diethyl ether or THF. Yield: 0.092 g (85%). ^{31}P{^{1}H} NMR (CH_2Cl_2): 2.6 (s with satellites, $J_{Pt-P} = 3771$ Hz). ^{1}H NMR (CD_2Cl_2): 7.75−7.48 (m, 20H, Ph), 2.23 (t, $^3J_{P-H} = 12.5$ Hz, 3H, N−Me). Anal. Calcd (found) for $C_{25}H_{23}N_3O_6P_2Pt$: C, 41.79 (42.20); H, 3.23 (3.29); N, 5.85 (5.85).

[(dppip)Pt(μ-NHPh)]$_2$(BF$_4$)$_2$ (4) (L$_2$ = dppip; Ar = Ph). To a stirred suspension of $[Pt(\mu\text{-OH})(dppip)]_2(BF_4)_2 \cdot 0.5CH_2Cl_2$ (0.100 g, 0.0683 mmol) in 5 mL of CH_2Cl_2 is added aniline (0.035 g, 0.38 mmol) in 2 mL of CH_2Cl_2. The resulting homogeneous solution is stirred for 5 h. The solution is then concentrated and the white solid product precipitated by layering the solution with diethyl ether. Yield: 0.095 g (88%). ^{31}P{^{1}H} NMR (CH_2Cl_2): −21.9 (s with satellites, $J_{Pt-P} = 2843$ Hz). ^{1}H NMR (CD_2Cl_2): 7.84−7.48 (m, 40H, Ph), 6.3 (v br s, 4H, NPh), 5.98−5.88 (m, 6H, NPh), 4.41 (br t, $^1J_{N-H} = 5$ Hz, 2H, NH), 1.12 (t, $^3J_{P-H} = 15.0$ Hz, 6H, CMe_2), 0.93 (t, $^3J_{P-H} = 15.0$ Hz, 6H, CMe_2). Anal. Calcd (found) for $C_{66}H_{64}B_2F_8N_2P_4Pt_2$: C, 50.37 (49.98); H, 4.10 (4.27); N, 1.78 (2.02).

[L$_2$Pt(μ-NH-4-tol)]$_2$(BF$_4$)$_2$ (4) (L$_2$ = dppip, dppma; Ar = Ph). To a stirred suspension of $[L_2Pt(\mu\text{-OH})]_2(BF_4)_2$ (0.100 g, ∼0.07 mmol) in 5 mL of CH_2Cl_2 is added 4-toluidine (0.035 g, 0.33 mmol) in 2 mL of CH_2Cl_2. The resulting homogeneous solution is stirred for 5 h (dppma) or heated at 50 °C for 1 h (dppip). The solution is then concentrated and the white solid product precipitated with diethyl ether. The dppip product precipitates with toluidine, which can be removed by recrystallization from CH_2Cl_2/Et_2O. Yield: 80−85% (∼0.09 g). dppip: ^{31}P{^{1}H} NMR (CH_2Cl_2) −22.0 (s with satellites, $J_{Pt-P} = 2841$ Hz); ^{1}H NMR (CD_2Cl_2, 250 MHz, 27 °C) 7.83−7.43 (m, 40H, Ph), 6.20 (br s, 4H, tol), 5.66 (d, $^3J_{H-H} = 8.0$ Hz, 4H, tol), 4.43 (br t, $^1J_{N-H} = 5$ Hz, 2H, NH), 1.71 (s, 6H, tol), 0.99 (t, $^3J_{P-H} = 15.0$ Hz, 12H, CMe_2); ^{1}H NMR (CD_2Cl_2, 300 MHz, −70 °C) 7.64−7.33 (m, 40H, Ph), 6.36 (d, $^3J_{H-H} = 5$ Hz, 2H, tol), 5.76 (d, $^3J_{H-H} = 5$ Hz, 2H, tol), 5.67 (d, $^3J_{H-H} = 5$ Hz, 2H, tol), 5.36 (d, $^3J_{H-H} = 5$ Hz, 2H, tol), 4.45 (br s, 2H, NH), 1.66 (s, 6H, tol), 0.95 (t, $^3J_{P-H} = 15$ Hz, 6H, CMe_2), 0.89 (t, $^3J_{P-H} = 15$ Hz, 6H, CMe_2). Anal. Calcd (found) for $C_{68}H_{68}B_2F_8N_2P_4Pt_2$: C, 51.02 (51.07); H, 4.28 (4.19); N, 1.75 (2.13). dppma: ^{31}P{^{1}H} NMR (CH_2Cl_2) 19.6 (s with satellites, $J_{Pt-P} = 2979$ Hz); ^{1}H NMR (CD_2Cl_2, 250 MHz, 27 °C) 7.75−7.19 (m, 40H, Ph), 6.37 (br d, $^3J_{H-H} = 7.5$ Hz, 4H, tol), 5.81 (br s, 4H, tol), 4.64 (br t, $^1J_{N-H} = 5$ Hz, 2H, NH), 2.13 (t, $^3J_{P-H} = 10.0$ Hz, 6H, NMe), 2.04 (s, 6H, tol). ^{1}H NMR (CD_2Cl_2, 250 MHz, −75 °C) 7.72−7.23 (m, 40H, Ph), 6.54 (d, $^3J_{H-H} = 7.5$ Hz, 2H, tol), 6.34 (d, $^3J_{H-H} = 7.5$ Hz, 2H, tol), 6.24 (d, $^3J_{H-H} = 7.5$ Hz, 2H, tol), 5.38 (d, $^3J_{H-H} = 7.5$ Hz, 2H, tol), 4.53 (br s, 2H, NH), 2.09 (t, $^3J_{P-H} = 10.0$ Hz, 6H, NMe), 1.99 (s, 6H, tol); IR (thin film) 3250 cm^{-1} (N−H). Anal. Calcd (found) for $C_{64}H_{62}B_2F_8N_4P_4Pt_2 \cdot 1.5CH_2Cl_2$: C, 46.22 (46.28); H, 3.85 (3.89); N, 3.29 (3.25).

[(dppip)$_2$Pt$_2$(μ-NH-2,6-xylyl)(μ-OH)](BF$_4$)$_2$ (5). To a stirred solution of $[Pt(\mu\text{-OH})(dppip)]_2(BF_4)_2 \cdot 0.5CH_2Cl_2$ (0.100 g, 0.0683 mmol) in 5 mL of CH_2Cl_2 is added 2,6-dimethylaniline (0.037 g, 0.30 mmol). The homogeneous solution is stirred overnight, concentrated under reduced pressure, and layered with diethyl ether to obtain the white crystalline product. Yield: 0.070 g (64%). ^{31}P-{^{1}H} NMR (CH_2Cl_2): −29.6 (d, $^1J_{Pt-P} = 3248$ Hz, $^2J_{P-P} = 60$ Hz), −22.8 (d, $^1J_{Pt-P} = 2771$ Hz, $^2J_{P-P} = 60$ Hz). ^{1}H NMR (CD_2Cl_2): 8.31−6.58 (m, 40H, Ph), 6.02 (d, $^3J_{H-H} = 7.5$ Hz, 1H, xylyl), 5.95 (t, $^3J_{H-H} = 7.5$ Hz, 1H, xylyl), 5.59 (d, $^3J_{H-H} = 7.5$ Hz, 1H, xylyl), 4.61 (br, s, NH), 3.32 (s, 3H, xylyl-CH_3), 2.34 (br s, OH), 1.64 (s, 3H, xylyl-CH_3), 1.37 (t, $^3J_{P-H} = 15.0$ Hz, 6H, CMe_2), 0.76 (t, $^3J_{P-H} = 15.0$ Hz, 6H, CMe_2). Anal. Calcd (found) for $C_{62}H_{63}B_2F_8NOP_4Pt_2 \cdot CH_2Cl_2$: C, 46.98 (46.94); H, 4.07 (4.41); N, 0.87 (1.30).

[(dppma)Pt(NH$_2$-2,6-xylyl)$_2$](NO$_3$)$_2$ (6). To a stirred suspension of $[Pt(NO_3)_2(dppma)]$ (0.100 g, 0.139 mmol) in 3 mL of CH_2Cl_2 is added 2,6-dimethylaniline (0.075 g, 0.62 mmol) in 2 mL of CH_2Cl_2. The homogeneous solution is stirred overnight and layered with an equal amount of toluene to obtain the pure white solid product. Yield: 0.090 g (67%). ^{31}P{^{1}H} NMR (CH_2Cl_2): 3.0 (br, s with satellites, $J_{Pt-P} = 3810$ Hz). (The ^{31}P{^{1}H} NMR spectrum of the reaction mixture shows a broad signal at 13.6 ppm ($J_{Pt-P} = 3222$ Hz)). ^{1}H NMR ($CDCl_3$): 7.78−7.56 (m, 20H, Ph), 6.89 (d, $^3J_{H-H} = 7.50$ Hz, 4H, xylyl), 6.59 (t, $^3J_{H-H} = 7.5$ Hz, 2H, xylyl), 4.62 (s, br, NH_2), 2.34 (t, $^3J_{P-H} = 12.5$ Hz, 3H, N−Me), 2.16 (s, 12H, xylyl-CH_3). Anal. Calcd (found) for $C_{41}H_{45}N_5O_6P_2Pt$: C, 51.24 (51.20); H, 4.72 (4.69); N, 7.29 (7.19).

[{Pt(μ-N-4-tol)(dppma)}$_2$·Li(DME)](BF$_4$) (9). $LiN(SiMe_3)_2$ (0.050 g, 0.30 mmol) in 5 mL of DME is added dropwise to a stirred suspension of $[Pt(\mu\text{-NH-4-tol})(dppma)]_2(BF_4)_2$ (0.100 g, 0.0635 mmol) in 10 mL of DME. The suspension of the diamido complex initially turns yellow but becomes an orange solution after complete addition. The orange solution is stirred for 1 h, concentrated, and then stored at −30 °C to obtain the yellow crystalline product. Crystals for the X-ray analysis were obtained by dissolving the product in a DME solution of $LiN(SiMe_3)_2$ and cooling the mixture to −30 °C. Yield: 0.070 g (70%). ^{31}P{^{1}H} NMR (DME): 28.9 (s with satellites, $^1J_{Pt-P} = 2792$ Hz, $^2J_{Pt-P} = 81$ Hz). ^{1}H NMR (CD_2Cl_2, 0 °C): 7.67−7.08 (m, 40H, Ph), 6.27 (d, $^3J_{H-H} = 7.5$ Hz, 4H, tol), 6.00 (d, $^3J_{H-H} = 7.5$ Hz, 4H, tol), 3.52 (s, 4H, DME), 3.01(s, 6H, DME), 2.17 (t, $^3J_{P-H} = 12.5$ Hz, 6H, NMe), 2.07 (s, 6H, tol).

[Pt(μ-NPh)(dppip)]$_2$·LiN(SiMe$_3$)$_2$ (10) (M = Pt, Ar = Ph). $LiN(SiMe_3)_2$ (0.050 g, 0.30 mmol) in 5 mL of THF is added dropwise to a stirred suspension of $[Pt(\mu\text{-NHPh})(dppip)]_2(BF_4)_2$ (0.100 g, 0.0636 mmol) in 10 mL of THF. On addition of the base, the colorless suspension slowly turns yellow, and after complete addition, a clear yellow solution is obtained. The yellow solution is stirred for an additional 1 h, concentrated under reduced pressure, layered with an equal volume of petroleum ether, and cooled to −30 °C to obtain yellow prismatic crystals. Yield: 0.070 g (71%). ^{31}P{^{1}H} NMR (THF): −12.8 (s with satellites, $^1J_{Pt-P} = 2753$ Hz, $^2J_{Pt-P} = 60$ Hz). ^{1}H NMR (CD_2Cl_2): 7.85−7.15 (m, 40H, Ph), 6.43 (d, $^3J_{H-H} = 7.5$ Hz, 4H, NPh), 5.79 (t, $^3J_{H-H} = 7.5$ Hz, 4H, NPh), 5.32 (t, $^3J_{H-H} = 7.5$ Hz, 2H, NPh), 0.95 (t, $^3J_{P-H} = 15.0$ Hz, 6H, CMe_2), 0.73 (t, $^3J_{P-H} = 15.0$ Hz, 6H, CMe_2), 0.06 (s, 18H, $N(SiMe_3)_2$).

[Pt(μ-N-4-tol)(dppip)]$_2$·LiN(SiMe$_3$)$_2$ (10) (M = Pt, Ar = 4-tol). The procedure is the same as for the Ph derivative. Yield: 0.080 (81%) of yellow prismatic crystals. Crystals for the X-ray analysis were obtained as described for the Ph derivative. ^{31}P{^{1}H} NMR (THF): −12.8 (s with satellites, $^1J_{Pt-P} = 2758$ Hz, $^2J_{Pt-P} = 60$ Hz). ^{1}H NMR (CD_2Cl_2): 7.85−7.16 (m, 40H, Ph), 6.27 (d, $^3J_{H-H} = 7.5$

Hz, 4H, tol), 5.56 (d, $^3J_{H-H}$ = 7.50 Hz, 4H, tol), 1.82 (s, 6H, tol), 0.95 (t, $^3J_{P-H}$ = 15.0 Hz, 6H, CMe_2), 0.86 (t, $^3J_{P-H}$ = 15.0 Hz, 6H, CMe_2), 0.02 (s, 18H, $N(SiMe_3)_2$). Anal. Calcd (found) for $C_{74}H_{84}LiN_3P_4Pt_2Si_2$: C, 55.81 (54.29, 52.05); H, 5.32 (5.75, 5.21); N, 2.64 (2.38, 2.15). The low analysis results suggest entrainment of $LiBF_4$ in the bulk samples or partial hydrolysis of these very air sensitive samples.

[Pt(*μ*-N-2,6-xylyl)(dppma)]$_2$·LiNO$_3$ (11) (M = Pt). $LiN(SiMe_3)_2$ (0.064 g, 0.38 mmol) in 5 mL of DME is added dropwise to a stirred suspension of $[Pt(NH_2\text{-}2,6\text{-xylyl})(dppma)](NO_3)_2$ (0.100 g, 0.104 mmol) in 10 mL of DME. The suspension of the diamido complex initially turns yellow but becomes an orange solution after the addition is complete. The orange solution is stirred for 1 h and then stored at −30 °C to obtain the orange crystalline product. Crystals for the X-ray analysis were obtained from THF as described for **10**. Yield: 0.040 g (51%). $^{31}P\{^1H\}$ NMR (DME): 28.0 (s with satellites, $^1J_{Pt-P}$ = 2729 Hz). ^1H NMR (CD_2Cl_2, −20 °C): 7.78−7.56 (m, 40H, Ph), 6.89 (d, $^3J_{H-H}$ = 7.5 Hz, 4H, xylyl), 6.59 (t, $^3J_{H-H}$ = 7.50 Hz, 2H, xylyl), 3.52 (s, 4H, DME), 3.01 (s, 6H, DME), 2.17 (t, $^3J_{P-H}$ = 12.5 Hz, 6H, NMe), 2.07 (s, 12H, xylyl-CH_3). Anal. Calcd (found) for $C_{66}H_{64}N_4P_4Pt_2\cdot 2LiNO_3\cdot C_4H_{10}O_2$: C, 50.79 (50.68); H, 4.51 (4.72); N, 5.08 (4.44).

[Pt$_2$(*μ*-N-2,6-xylyl)(*μ*-O)(dppip)$_2$]·LiN(SiMe$_3$)$_2$·LiBF$_4$ (12). $LiN(SiMe_3)_2$ (0.050 g, 0.30 mmol) in 4 mL of THF is added dropwise to a stirred suspension of $[Pt_2(\mu\text{-NH-}2,6\text{-xylyl})(\mu\text{-OH})(dppip)_2](BF_4)_2$ (0.160 g, 0.105 mmol) in 10 mL of THF. On addition of the base, the colorless suspension slowly becomes yellow, and after complete addition, a clear yellow solution forms. The yellow solution is stirred for an additional 1 h and then concentrated under reduced pressure, layered with equal amount of petroleum ether, and cooled to −30 °C to obtain the yellow crystalline product. Yield: 0.100 g (59%). $^{31}P\{^1H\}$ NMR (THF): −12.3 (d with satellites, $^1J_{Pt-P}$ = 3039 Hz, $^2J_{P-P}$ = 41 Hz, P trans to oxo), −22.8 (d with satellites, $^1J_{Pt-P}$ = 2571 Hz, $^2J_{P-P}$ = 41 Hz, P trans to imido). ^1H NMR (CD_2Cl_2): 8.59−7.14 (m, 40H, Ph), 6.28 (br d, $^3J_{P-H}$ = 7.5 Hz, 2H, xylyl) 6.02 (br t, $^3J_{P-H}$ = 7.5 Hz, 1H, xylyl), 2.1(br, s, 6H, xylyl), 1.18 (t, $^3J_{P-H}$ = 15.0 Hz, 12H, CMe_2), 0.05 (s, 18H, $N(SiMe_3)_2$). $^{19}F\{^1H\}$ NMR (THF): −154.1 (s, BF_4). Anal. Calcd (found) for $C_{68}H_{79}BF_4N_2OSi_2Li_2P_4Pt_2$: C, 50.67 (50.18); H, 4.94 (4.77); N, 1.74 (1.76).

[Pt(*μ*-N-4-tol)(dppip)]$_2$·*n*NaBF$_4$. $NaN(SiMe_3)_2$ (0.055 g, 0.30 mmol) in 5 mL of THF is added dropwise to a stirred suspension of $[Pt(\mu\text{-NH-}4\text{-tol})(dppip)]_2(BF_4)_2$ (0.100 g, 0.0625 mmol) in 10 mL of THF. The colorless suspension, on addition of the base, slowly turns yellow, and after complete addition, a clear yellow solution is obtained. The yellow solution is stirred for an additional 1 h, concentrated under reduced pressure, layered with an equal volume of petroleum ether, and cooled to −30 °C to obtain the orange-yellow crystalline product. Yield: 0.065 g (68%, assuming n = 1). $^{31}P\{^1H\}$ NMR (THF): −13.2 (s with satellites, $^1J_{Pt-P}$ = 2707 Hz). ^1H NMR (CD_2Cl_2, 0 °C): 7.85−7.17 (m, 40H, Ph), 6.27 (d, $^3J_{P-H}$ = 7.5 Hz, 4H, tol), 5.56 (d, $^3J_{P-H}$ = 7.5 Hz, 4H, tol), 1.82 (s, 6H, tol), 0.95 (t, $^3J_{P-H}$ = 15.0 Hz, 6H, CMe_2), 0.86 (t, $^3J_{P-H}$ = 15.0 Hz, 6H, CMe_2). ^{19}F NMR (THF): −156.2 (s).

[Pt(*μ*-oxo)(dppip)]$_2$·LiN(SiMe$_3$)$_2$·2LiBF$_4$ (13). $LiN(SiMe_3)_2$ (0.050 g, 0.30 mmol) in 5 mL of THF is added dropwise to a stirred suspension of $[Pt(\mu\text{-OH})(dppip)]_2(BF_4)_2$ (0.100 g, 0.064 mmol) in 10 mL of THF. The resulting pale yellow solution is allowed to stir for an additional 20 min and then concentrated in vacuo. Layering the concentrated solution with petroleum ether and storing at −30 °C yields the pale yellow solid product. Yield: 0.060 g (59%). $^{31}P\{^1H\}$ NMR (THF): −23.2 (br s with satellites, $^1J_{Pt-P}$ = 3008 Hz). ^1H NMR (CD_2Cl_2): 8.24−7.55 (br m, 40H, Ph), 1.07 (br t, 12H, $^3J_{P-H}$ = 15 Hz, CMe_2), 0.02 (br s, 36H, $N(SiMe_3)_2$). Anal. Calcd (found) for $C_{54}H_{52}O_2P_4Pt_2\cdot LiNSi_2C_6H_{18}\cdot 2LiBF_4$: C, 44.99 (44.99); H, 4.40 (4.12); N, 0.87 (0.68).

[Pt(*μ*-O)(dppip)]$_2$·*n*MBF$_4$ (M = Na or K). $MN(SiMe_3)_2$ (0.055 g, M = Na; 0.60 g, M = K, 0.30 mmol) in 5 mL of THF is added dropwise to a stirred suspension of $[Pt(\mu\text{-OH})(dppip)]_2(BF_4)_2$ (0.100 g, 0.0703 mmol) in 10 mL of THF. The resulting pale yellow solution is allowed to stir for an additional 20 min. Layering the solution with petroleum ether and storing at −30 °C yields the pale yellow solid product. Yield (assuming n = 1): M = Na, 0.055 g (58%, assuming n = 1); M = K, 0.050 g (52%, assuming n = 1). Spectroscopic data are the same for both derivatives. $^{31}P\{^1H\}$ NMR (THF): −24.2 (s with satellites, $^1J_{Pt-P}$ = 2950 Hz). ^1H NMR (CD_2Cl_2): 8.24−7.55 (m, 40H, Ph), 1.30 (t, 12H, $^3J_{P-H}$ = 15.0 Hz, CMe_2). ^{19}F NMR (THF): −156.2 (s).

Palladium Complexes. Reaction of PdCl$_2$(dppma) with AgNO$_3$. To a stirred suspension of $PdCl_2$(dppma) (0.100 g, 0.173 mmol) in 8 mL of CH_2Cl_2 is added solid $AgNO_3$ (0.060 g, 0.35 mmol) in portions. The mixture is stirred for 3 h. The AgCl precipitate is removed by filtration through diatomaceous earth. The resulting clear filtrate is concentrated under reduced pressure, and a lemon-yellow solid is precipitated with diethyl ether (0.070 g). ^{31}P NMR spectroscopy of the reaction mixtures and the dissolved isolated solid indicates the presence of a mixture of compounds. $^{31}P\{^1H\}$ NMR (CH_2Cl_2): 32.7 (d, $^2J_{P-P}$ = 21 Hz), 26.5 (d, $^2J_{P-P}$ = 21 Hz), 29.1 (s). ^1H NMR (CD_2Cl_2): 7.79−7.61 (m, 20H, Ph), 2.56 (t, $^3J_{P-H}$ = 12.5 Hz, 3H, N−Me).

Reaction of PdCl$_2$(dppma) with AgX (X = BF$_4$, OTf). To a stirred CH_2Cl_2 (8 mL) suspension of $PdCl_2$(dppma) (0.100 g, 0.174 mmol) containing one drop of water is added AgX (0.365 mmol) in solid portions. After complete addition, the reaction mixture is stirred for 1 h in the dark and the AgCl precipitate is removed by filtration through diatomaceous earth. The resulting clear orange solution is concentrated under reduced pressure and the yellow product precipitated with diethyl ether. Yield for X = BF_4: 0.060 g. Crystals of $Pd(OTf)_2$(dppma) for the X-ray analysis were obtained by layering the concentrated mixture with diethyl ether. $^{31}P\{^1H\}$ NMR (CH_2Cl_2): 26.1 (s). ^1H NMR (CD_2Cl_2): 7.85−7.35 (m, 40H, Ph), 4.34 (br s, OH), 2.70 (t, $^3J_{P-H}$ = 12.50 Hz, 6H, N-Me). Anal. Found: C, 4.18; H, 3.41; N, 2.06. X = OTf**:** yield 0.070 g; $^{31}P\{^1H\}$ NMR (CH_2Cl_2) 26.5 (s); ^1H NMR (CD_2Cl_2) 7.82−7.62 (m, 40H, Ph), 2.66 (t, $^3J_{P-H}$ = 12.50 Hz, 6H, N−Me). Anal. Found: C, 44.04; H, 3.53; N, 2.08.

Pd(OTf)$_2$(dppip) (3). To a stirred CH_2Cl_2 (8 mL) suspension of $PdCl_2$(dppip) (0.100 g, 0.170 mmol) is added AgOTf (0.090 g, 0.35 mmol) in solid portions. After the addition of AgOTf, the reaction mixture is stirred for 1 h in the dark and the AgCl precipitate is removed by filtration through diatomaceous earth. The resulting clear green solution is concentrated under reduced pressure, and the pale yellow solid product is precipitated with diethyl ether. Yield: 0.110 g (79%). $^{31}P\{^1H\}$ NMR (CH_2Cl_2): −16.5 (s). ^1H NMR (CD_2Cl_2): 8.08−7.57(m, 20H, Ph), 1.37 (t, $^3J_{P-H}$ = 15.0 Hz, 6H, CMe_2). Anal. Calcd (found) for $C_{29}H_{26}F_6O_6P_2PdS_2$: C, 42.63 (42.36); H, 3.20 (3.06).

[Pd(NH$_2$-4-tol)$_2$(dppip)](OTf)$_2$ (7) (L$_2$ = dppip, X = OTf). To a stirred suspension of $Pd(OTf)_2$(dppip) (0.100 g, 0.123 mmol) in 8 mL of CH_2Cl_2 is added 4-toluidine (0.035 g, 0.33 mmol) in 2 mL of CH_2Cl_2. The resulting homogeneous yellow solution is stirred for 2 h, after which time the solution is concentrated and the yellow product precipitated with diethyl ether. Yield: 0.100 g (80%). Crystals for the X-ray analysis were obtained by layering a concentrated CH_2Cl_2 solution with diethyl ether. $^{31}P\{^1H\}$ NMR (CH_2Cl_2): −13.1 (s). ^1H NMR ($CDCl_3$): 8.01−7.54 (m, 20H, Ph),

6.82 (d, $^3J_{H-H}$ = 7.5 Hz, 4H, tol), 6.25 (d, $^3J_{H-H}$ = 7.5 Hz, 4H, tol), 5.85 (br s, 4H, NH_2), 1.98 (s, 6H, tol), 1.08 (t, $^3J_{P-H}$ = 15.0 Hz, 6H, CMe_2). Anal. Calcd (found) for $C_{43}H_{44}F_6N_2O_6P_2PdS_2 \cdot CH_2Cl_2$: C, 47.34 (47.19); H, 4.15 (4.23), N, 2.51 (2.56).

[Pd(NH$_2$-4-tol)$_2$(dppma)](X)$_2$ (7) (L$_2$ = dppma, X = BF$_4$, OTf). To a stirred suspension of (dppma)$PdCl_2$ (0.100 g, 0.174 mmol) in 10 mL of CH_2Cl_2 is added AgX (X = BF_4, 0.071 g; X = OTf, 0.094 g; 0.36 mmol). The mixture is stirred for 2 h. The AgCl precipitate is removed by filtration through diatomaceous earth. The resulting clear filtrate is concentrated under reduced pressure to 3 mL, and to this clear solution is added 4-toluidine (0.040 g, 0.37 mmol) in 2 mL of CH_2Cl_2. The homogeneous solution is stirred for 3 h and layered with an equal amount of Et_2O to obtain the yellow solid product. Crystallization from CH_2Cl_2/Et_2O gives analytically pure products. Crystals for the X-ray analysis were obtained by layering a concentrated CH_2Cl_2 solution with toluene. X = BF_4**:** yield 0.090 g (58%); $^{31}P\{^1H\}$ NMR (CH_2Cl_2) 32.0 (s); ^1H NMR ($CDCl_3$) 7.73−7.41 (m, 20H, Ph), 6.90 (d, $^3J_{H-H}$ = 7.5 Hz, 4H, tol), 6.52 (d, $^3J_{H-H}$ = 7.5 Hz, 4H, tol), 5.85 (br s, 4H, NH_2), 2.23 (t, $^3J_{P-H}$ = 12.5 Hz, 3H, NMe), 2.15 (s, 6H, tol). Anal. Calcd (found) for $C_{39}H_{41}B_2F_8N_3P_2Pd$: C, 52.34 (51.95); H, 4.62 (4.61); N, 4.70 (4.52). X = OTf: yield 0.095 g (54%); $^{31}P\{^1H\}$ NMR (CH_2Cl_2) 32.4 (s); ^1H NMR ($CDCl_3$) 7.74−7.48 (m, 20H, Ph), 6.89 (d, $^3J_{H-H}$ = 7.5 Hz, 4H, tol), 6.53 (d, $^3J_{H-H}$ = 7.5 Hz, 4H, tol), 6.28 (br s, 4H, NH_2), 2.23 (t, $^3J_{P-H}$ = 12.5 Hz, 3H, NMe), 2.10 (s, 6H, tol). Anal. Calcd (found) for $C_{41}H_{41}F_6N_3O_6P_2PdS_2$: C, 48.37 (48.37); H, 4.06 (4.03); N, 4.13 (4.14).

[(dppma)Pd(NH$_2$-2,6-xylyl)$_2$](NO$_3$)$_2$ (8). To a stirred suspension of (dppma)$PdCl_2$ (0.100 g, 0.174 mmol) in 10 mL of CH_2Cl_2 is added $AgNO_3$ (0.060 g, 0.35 mmol). The mixture is stirred for 3 h. The AgCl precipitate is removed by filtration through diatomaceous earth. The resulting clear filtrate is concentrated under reduced pressure to 3 mL, and to this clear solution is added 2,6-dimethylaniline (0.085 g, 0.69 mmol) in 2 mL of CH_2Cl_2. The homogeneous solution is stirred overnight and layered with an equal amount of toluene to obtain the deep yellow solid product. Yield: 0.120 g (79%). $^{31}P\{^1H\}$ NMR (CH_2Cl_2): 26.7 (s). ^1H NMR (CD_2Cl_2): 7.77−7.52 (m, 20H, Ph), 6.82 (d, $^3J_{H-H}$ = 7.5 Hz, 4H, *m*-xylyl-H), 6.50 (t, $^3J_{H-H}$ = 7.5 Hz, 2H, *p*-xylyl-H), 3.62 (br s, 4H, NH_2), 2.40 (t, $^3J_{P-H}$ = 12.5 Hz, 3H, N-Me), 2.08 (s, 12H, 2,6-Me_2). Anal. Calcd (found) for $C_{41}H_{45}N_5O_6P_2Pd$: C, 56.47 (56.26); H, 5.21 (5.40); N, 8.04 (8.12).

[{Pd(μ-N-4-tol)(dppma)}$_2$·Li(DME)](X) (9) (M = Pd; Ar = 4-tol; X = BF$_4$, OTf). $LiN(SiMe_3)_2$ (0.066 g, 0.39 mmol) in 5 mL of DME was added dropwise to a stirred suspension of [Pd(NH$_2$-4-tol)$_2$(dppma)](X)$_2$ (0.100 g) in 10 mL of DME. On addition of base, the suspension slowly turns from yellow to orange and then to red, and after complete addition the mixture becomes a deep red solution. The deep red solution is stirred for 1 h, concentrated, and stored at −30 °C to obtain the red solid product. X = BF_4: yield 0.040 g (51%); $^{31}P\{^1H\}$ NMR (DME) 50.7 (s); ^1H NMR (CD_2Cl_2, −20 °C) 7.58−6.94 (m, 40H, Ph), 6.26 (d, $^3J_{H-H}$ = 7.5 Hz, 4H, tol), 5.30 (d, $^3J_{H-H}$ = 7.5 Hz, 4H, tol), 3.52 (s, 4H, DME), 3.01 (s, 6H, DME), 2.17 (t, $^3J_{P-H}$ = 12.5 Hz, 6H, NMe), 2.07 (s, 6H, tol). X = OTf: yield 0.040 g (56%); $^{31}P\{^1H\}$ NMR (DME) 52.1 (s); ^1H NMR (CD_2Cl_2, −20 °C) 7.58−6.95 (m, 40H, Ph), 6.42 (d, $^3J_{H-H}$ = 7.5 Hz, 4H, tol), 5.90 (d, $^3J_{H-H}$ = 7.5 Hz, 4H, tol), 3.50 (s, 4H, DME), 3.12 (br s, 6H, DME), 2.21 (br t, $^3J_{P-H}$ = 12.5 Hz, 6H, NMe), 2.05 (s, 6H, tol). Anal. Calcd (found) for $C_{69}H_{70}F_3LiN_4O_5P_4SPd_2$: C, 51.24 (51.20); H, 4.81 (4.79); N, 3.88 (3.95).

[Pd(μ-N-4-tol)(dppip)]$_2$·LiN(SiMe$_3$)$_2$ (10) (M = Pd, Ar = 4-tol). To the stirred suspension of [Pd(NH$_2$-4-tol)$_2$(dppip)](OTf)$_2$ (0.100 g, 0.0971 mmol) in 5 mL of THF was added dropwise LiN(SiMe$_3$)$_2$ (0.045 g, 0.27 mmol) in 2 mL of THF. The yellow suspension of amine complex on addition of the base slowly changed in to red and after the complete addition turned in to a clear deep red solution. The red solution was stirred for additional 1 h for the completion of deprotonation, concentrated under reduced pressure, layered with an equal amount of petroleum ether, and cooled to −30 °C to obtain red prismatic crystals. Crystals for the X-ray analysis were obtained in this way. Yield: 0.045 g, 65%. $^{31}P\{^1H\}$ NMR (THF): 8.6 (s). ^1H NMR (CD_2Cl_2, 0 °C): 7.76−7.14 (m, 40H, Ph), 6.53 (d, $^3J_{H-H}$ = 7.5 Hz, 4H, tol), 5.60 (d, $^3J_{H-H}$ = 7.5 Hz, 4H, tol), 1.82 (s, 6H, tol), 0.89 (t, $^3J_{P-H}$ = 15 Hz, 6H, CMe_2), 1.18 (t, $^3J_{P-H}$ = 15 Hz, 6H, CMe_2), 0.05 (s, 18H, $N(SiMe_3)_2$).

[Pd(μ-N-4-tol)(dppip)]$_2$·*x*NaOTf. $NaN(SiMe_3)_2$ (0.050 g, 0.27 mmol) in 2 mL of THF was added dropwise to a stirred suspension of [Pd(NH$_2$-4-tol)$_2$(dppip)](OTf)$_2$ (0.100 g, 0.0971 mmol) in 5 mL of THF. The yellow suspension of amine complex on addition of the base slowly changed in to red and after the complete addition turned in to a clear deep red solution. The red solution was stirred for additional 1 h for the completion of deprotonation, concentrated under reduced pressure, layered with an equal amount of petroleum ether, and cooled to −30 °C to obtain the red crystalline product. Yield: 0.045 g, 65%. $^{31}P\{^1H\}$ NMR (THF): 9.2 (s). ^1H NMR (CD_2Cl_2, 0 °C): 7.76−7.14 (m, 40H, Ph), 6.53 (d,$^3J_{H-H}$ = 7.5 Hz, 4H, tol), 5.60 (d, $^3J_{H-H}$ = 7.5 Hz, 4H, tol), 1.82 (s, 6H, tol), 0.89 (t, $^3J_{P-H}$ = 15 Hz, 6H, CMe_2), 1.18 (t, $^3J_{P-H}$ = 15 Hz, 6H, CMe_2). ^{19}F NMR (THF): −78.9 (s, OTf).

[Pd(μ-N-2,6-xylyl)(dppma)]$_2$·LiNO$_3$ (11) (M = Pd). The procedure is the same as that used for the Pt analogue. Yield: 0.040 g (53%) of red crystals. $^{31}P\{^1H\}$ NMR (DME): 52.2 (s). ^1H NMR data could not be obtained as the complex is either insoluble or decomposes in all common deuterated NMR solvents (including cold CD_2Cl_2). Crystals for the X-ray analysis were grown as described for the Pt analogue.

Crystal Structure Analyses. Crystal data and refinement results are given in Tables 1 and 2. CIF files are supplied as Supporting Information. Crystals were grown as described in the syntheses given above and were mounted by pipetting the crystals and mother liquor into a pool of heavy oil. A suitable crystal was selected and removed from the oil with a glass fiber. With the oil-covered crystal adhering to the end of the glass fiber the sample was transferred to an N_2 cold stream on the diffractometer and data were collected at −100 °C. Data reduction and processing followed routine procedures. Structures were solved by direct methods and refined on F_o^2.

Acknowledgment. This work was supported by the Division of Chemical Sciences, Office of Basic Energy Sciences, Office of Energy Research, U.S. Department of Energy (Grant DE-FG02-88ER13880). A grant from the National Science Foundation (9221835) provided a portion of the funds for the purchase of the NMR equipment. We thank Dr. Charles Barnes and Dr. Alan James for assistance with the crystal structure determinations.

Supporting Information Available: Crystallographic information files (CIF) for structures **2**, **7** (L_2 = dppma, dppip), **9**−**11**, and $Pd(OTf)_2$(dppma). This material is available free of charge via the Internet at http://pubs.acs.org.

IC025987F